DESIGN OF LOCALIZED SURFACE PLASMON RESONANCE (LSPR) BASED BIOSENSOR FOR DETECTING A POTENTIAL CANCER BIOMARKER

A Thesis Submitted to
the Graduate School of
İzmir Institute of Technology
in Partial Fulfillment of the Requirements for the Degree of

MASTER OF SCIENCE

in Bioengineering

by
Cansu SÖYLEMEZ

July, 2020
İZMİR

ACKNOWLEDGEMENTS

The work presented in this thesis would not have been possible without the support of some people. Firstly, I would like to acknowledge my advisor Prof. Dr. Volga BULMUŞ for her guidance. She always shared her knowledge and helped me throughout my thesis. I greatly appreciate her support. I would like to thank my labmates Gürbüz DURSUN, Ecem ÖNAL, Aykut ZELÇAK, former labmates İlknur TAŞYÜREK and Aysel TOMAK for exchanging ideas and for being good friends. I would like to express my deepest thanks to Damla TAYKOZ who is also one of my labmates. Her assistance with the experiments and our brainstorming moments were priceless to me.

I want to thank my best friends Elçin MORGÜL and Işıl DİRİL who are always there whenever I need them. They backed me up all the time and motivated me to focus on my studies. I am thankful to my boyfriend Erel PEZÜK, for his continuous encouragement and emotional support.

I am indebted to my parents. They have always been an inspiration for me. I express my deepest gratitude to them for their unconditional and endless support.

ABSTRACT

DESIGN OF LOCALIZED SURFACE PLASMON RESONANCE (LSPR) BASED BIOSENSOR FOR DETECTING A POTENTIAL CANCER BIOMARKER

Conventional methods for detection of cancer are invasive, expensive and not suitable for early diagnosis. Therefore, demand for simple, sensitive and rapid biosensors for detection of cancer have been enormous. Gold nanorods (GNRs) have been ideal materials for utilization in biosensors because of their exceptional optical properties. Localized surface plasmon resonance (LSPR) which is created on GNR surface can be used for the development of label-free and sensitive biosensor systems. LSPR responds to changes in the refractive index of the surroundings and this change can be observed as the shift in the maximum absorption wavelengths. In this thesis, an LSPR based GNR biosensor was developed for sensitive detection of a sialic acid as a potential cancer biomarker. For this purpose, GNRs were synthesized at around 40-50 nm in length. Afterwards, glass surfaces were coated with GNRs and functionalized with self-assembling molecules. Specific monoclonal antibodies(Ab) were conjugated to the surface. The surface modifications were characterized via contact angle, scanning electron microscope, Fourier transform infrared spectroscopy and zeta potential. Ab-functionalized glass surfaces were used to quantitatively detect specific molecular bindings via LSPR. The sensitivity of the biosensor was determined as 281 RIU/nm. The detection limit in PBS was 1 nM, while in serum it was found to be as 10 nM because of the high protein content of serum. Control experiments showed that the developed biosensor chip was selective. The proposed system is promising for early diagnosis of cancer since it can detect a potential cancer biomarker at concentrations as low as nanomolar level.

ÖZET

POTANSİYEL BİR KANSER BELİRTECİNİN SAPTANMASI İÇİN LOKALİZE YÜZEY PLAZMON REZONANSI ESASLI BİYOSENSÖR TASARIMI

Kanser teşhisi için bilinen yöntemler invaziv ve maliyeti yüksek yöntemlerdir. Ayrıca erken teşhiste başarılı olamamaktadır. Bu sebeple güvenilir, hassas ve hızlı ölçüm sağlayabilen biyosensörlere ihtiyaç artmıştır. Altın nanoçubuklar eşsiz optik ve elektriksel özellikleriyle biyosensörlerde kullanmak için ideal bir malzemedir. Altın nanoçubukların yüzeyinde oluşan lokalize yüzey plazmon rezonansı (LSPR) ile etiket gerektirmeyen ve hızlı sonuç veren, hassas biyosensörler tasarlanabilmektedir. Lokalize yüzey plazmon rezonansı ortamın kırınım indisi değişimine göre yanıt vermektedir ve bu değişim ultraviyole-görünür ışık spektroskopisinde maksimum dalgaboyundaki pik kaymalarına bakarak gözlenebilmektedir. Bu çalışmada LSPR temelli altın nanoçubuk biyosensör tasarlanmıştır. Potansiyel kanser belirteci olarak bir sialik asit molekülünün teşhisi amaçlanmıştır. Bu amaç için öncelikle altın nanoçubuklar 40-50 nm boyutlarında sentezlenmiştir. Ardından, cam yüzeyler altın nanoçubuklar ile kaplanmış ve yüzey, spesifik moleküller ile fonksiyonelleştirilmiştir ve kanser belirtecine spesifik monoklonal antikor, yüzeye bağlanmıştır. Yüzey karakterizasyonları temas açı ölçümü, taramalı elekttron mikroskobu, Fourier dönüşümlü kızılötesi spektroskopisi ve zeta potansiyeli ölçümleri ile yapılmıştır. Antikor ile fonksiyonelleştirilmiş cam yüzeylerdeki spesifik moleküler bağlanmalar kantitatif olarak LSPR ile belirlenmiştir. Biyosensörün hassasiyeti 281 nm/RIU olarak bulunmuştur. Dedeksiyon limiti tampon çözeltide 1 nM, serumda ise yüksek protein içeriği sebebiyle 10 nM olarak bulunmuştur. Biyosensörün, teşhisi amaçlanan sialik asit molekülüne karşı seçiciliği kontrol deneyleriyle gösterilmiştir. Tasarlanan biyosensör, nanomolar seviyesi gibi düşük konsantrasyonlarda ölçüm sağlayabildiğinden kanserin erken teşhisi için umut verici bir sistemdir.

To my family…

TABLE OF CONTENTS

LIST OF FIGURES viii

CHAPTER 1. INTRODUCTION 1

CHAPTER 2. LITERATURE REVIEW 3

2.1. Biosensors and Their Applications 3

2.2. Types of Biosensors 6

2.3. LSPR Theory and Biosensing with LSPR 7

2.4. Gold Nanorods in Biosensing 9

2.5. Synthesis of Gold Nanorods 10

2.6. Surface Modification of Gold Nanorods 12

2.7. LSPR Based GNR Biosensors 13

2.8. GNR based LSPR Biosensors for Cancer Detection 15

CHAPTER 3. MATERIALS AND METHODS 19

3.1. Materials 19

3.2. Methods 20

3.2.1.Synthesis of GNRs 20

3.2.2.PEGylation of GNR solutions 20

3.2.3.Development of Biosensor Chips 21

3.2.4.Antigen Detection in PBS and Serum 22

3.2.5.Characterization of the Biosensor 23

3.2.5.1. Water Contact Angle Measurement 23

3.2.5.2. Scanning Electron Microscopy (SEM) 23

3.2.5.3. Fourier Transform Infrared (FTIR) Spectroscopy 23

3.2.5.4. Zeta Potential Measurement..... 23

CHAPTER 4. RESULTS AND DISCUSSION..... 24

4.1. GNR Synthesis and PEGylation 24

4.2. Preparation and Characterization of GNR Coated Glass Surfaces 26

4.3. Sensitivity of GNR Coated Glass Surfaces..... 29

4.4. Modification of GNR Coated Glass Surface 31

4.5. Control Experiments for Determination of Selectivity and Specificity.. 36

4.6. Antigen Detection in PBS and Serum..... 37

CHAPTER 5. CONCLUSION 42

REFERENCES ……...44

LIST OF FIGURES

Figure **Page**

Figure 2.1. Components of a biosensor 4
Figure 2.2. Comparison of LSPR and SPR principle 8
Figure 2.3. Mechanism of detection with an LSPR biosensor..... 8
Figure 2.4. Nanoparticle shape effect on LSPR spectra 9
Figure 2.5. Electron oscillations on a gold nanorod surface and LSPR spectra 10
Figure 2.6. Synthesis and reduction steps of GNRs 12
Figure 2.7. Fabrication of the gold nanorod sensor 15
Figure 2.8. Refractive index sensitivity test using solutions with different refractive indexes. Solutions were prepared with varying glycerol contents. Water (n=1.33) was taken as the starting point. 17
Figure 2.9. LSPR spectra and biosensor response upon detection of prostate cancer biomarker..... 18
Figure 4.1. LSPR spectra of synthesized GNRs 25
Figure 4.2. LSPR spectra of GNR before and after PEGylation 26
Figure 4.3. Water contact angle comparison of surfaces modified with different alkoxysilane molecules (AS1 and AS2). 27
Figure 4.4. SEM images of AS1 (A) and AS2 (B) modified and GNR coated glass surfaces.. 27
Figure 4.5. Before and after immobilization of GNRs onto glass substrates 28
Figure 4.6. LSPR spectra of GNRs after immobilization on a glass surface..... 29
Figure 4.7. SEM images of GNR coated surface after oxygen plasma 29
Figure 4.8. Refractive Index Sensitivity on LSPR spectra 30
Figure 4.9. Refractive index versus wavelength shift plot 30
Figure 4.10. Binding of SAMs on LSPR spectra..... 31
Figure 4.11. FTIR spectrum of plasma treated, no plasma applied and plasma treated SAM formed surfaces..... 32
Figure 4.12. Antibody binding on LSPR spectra..... 33
Figure 4.13. Effect of self-assembling molecules on preventing nonspecific bindings A) Antibody incubation without SAM and EDC/NHS B) Antibody incubation after SAM formation without EDC/NHS 35

Figure **Page**

Figure 4.14. Specificity of the antibody to the antigen on LSPR spectra 36

Figure 4.15. Antigen incorporation onto surface modified with non-specific IgG antibody. Antigen did not bind and no shift was observed on LSPR spectra. 37

Figure 4.16. Response of the biosensor in different complex media Response of the biosensor chip in different complex media. Chip surface after: SaM modification (purple); specific antibody conjugation (blue); treatment with cell culture medium without serum (green); treatment with cell culture medium with 10% (orange), 40% (dark orange), 100% (black) FBS. 38

Figure 4.17. LSPR spectra of specific antibody functionalized biosensor chips after treatment with PBS solutions having varying antigen concentrations 39

Figure 4.18. Antigen concentrations versus LSPR peak wavelength shifts determined for specific antibody functionalized biosensor chips after treatment with PBS solutions having varying antigen concentrations. The error bars represent standard deviation for measurements of 5 independent biosensor chips (n=5**)** 40

Figure 4.19. LSPR spectra of specific antibody functionalized biosensor chips after treatment with cell culture media having varying antigen concentrations 41

Figure 4.20. Antigen concentrations versus LSPR peak wavelength shifts determined for specific antibody functionalized biosensor chips after treatment with cell culture media having varying antigen concentrations. The error bars represent standard deviation for measurements of 5 independent biosensor chips (n=5). 41

ABBREVIATIONS

Symbol	Description
LSPR	Localized Surface Plasmon Resonance
CTAB	Cetyl Trimethyl Ammonium Bromide
SaM	Self-Assembled Monolayer
SEM	Scanning Electron Microscope
FTIR	Fourier Transform Infrared
OEG	Oligoethylene Glycol
UV-Vis	Ultraviolet-visible
LPB	Longitudinal Plasmon Band
TPB	Transverse Plasmon Band
AS	Alkoxysilane
PEG	Polyethylene glycol
GNRs	Gold nanorods
PBS	Phosphate buffered saline
RI	Refractive index
λ_{max}	Maximum wavelength
RIU	Refractive index unit
Ab	Antibody

CHAPTER 1

INTRODUCTION

Biosensors are systems which sense biological signals and convert these signals into detectable signals via a transducer. Biosensors involve a bioreceptor immobilized on the sensor surface which specifically recognizes a target analyte. This biorecognition creates a biological signal then it is converted and displayed on a processor. In the past decades, biosensors have emerged in biomedical applications as a consequence of increase in need for noninvasive, sensitive and accurate detection sytems (Erickson et al., 2008).

Localized surface plasmon based (LSPR) biosensors provide a label-free and sensitive detection by using optical properties of metal nanostructures. LSPR theory relies on changes of the refractive index of the environment. When a molecule binds to the surface of a metal nanoparticle, it alters the refractive index. This response can be tracked on the shift of the maximum absorption peak wavelength on UV-Vis spectra. Gold nanoparticles are well-known materials for utilization in LSPR-based biosensors. Gold is a chemically stable material. Itis resistant to oxidation. Moreover, refractive index sensitivity of gold nanoparticles is quite high especially when gold is used in nanorod shape. Gold nanorods (GNRs) present two plasmon bands which are transversal and longitudinal bands due to their LSPR properties. Longitudinal plasmon band (LPB) reacts to molecular bindings on the nanorods surface and gives information about the aspect ratio of GNRs.

For LSPR-based biosensor applications, GNRs can be used in either solution form or immobilized formon a substrate. Immobilization method is more favorable since GNRs on a substrate are more stable and controllable. Surface functionalization of GNRs is crucial to enable sensitive and selective receptor-analyte binding. Surface modification of GNRs generally takes place via strong gold-sulfur bond. Molecules immobilized on GNR surface create a self-assembled monolayer and provide further modifications such as antibody or protein conjugation. Oligo ethylene glycol (OEGs) are the best known SAM molecules to prevent nonspecific protein adsorption.

Cancer is among the leading causes of death in the World in the recent years. Traditional methods for detection of cancer are invasive,expensive and complicated. Moreover, these methods are not favorable for early diagnosis. Therefore, there is a need for trustworthy, sensitive, simple andlow-cost biosensing systems for detection of cancer. LSPR based GNR biosensors for cancer detection have been reported in some studies which are based on biorecognition of the specific cancer biomarker by immobilizing the recognition element on the GNR surface.

In the scope of this thesis, an LSPR based GNR biosensor platform was developed with the aim of detection of a sialic acid as a potential cancer biomarker. For this purpose, glass surfaces were silanized, and PEG stabilized GNRs were immobilized onto the glass surfaces. Afterwards, the surface was functionalized with self-assembling molecules. The monoclonal antibody which is specific to the target sialic acid was bound to the surface via EDC/NHS chemistry. The surface modifications were characterized via several techniques including contact angle, scanning electron microscope, Fourier transform infrared spectroscopy and zeta potential.

Ab-functionalized glass surfaces were used to quantitatively detect specific molecular bindings via LSPR. Sensitivity and selectivity of GNR-based biosensor platform were investigated through several different experiments. All the results presented in Chapter 5, Results and Discussion.

CHAPTER 2

LITERATURE REVIEW

2.1. Biosensors and Their Applications

Biosensors were first discovered in 1962 by Clark and Lyons to measure glucose levels in biological samples via an enzyme electrode. This biosensor was an electrochemical biosensor which was based on oxygen consumption by an enzymatic reaction (Clark and Lyons, 1962). Since then, different types of biosensors have been developed for various applications such as medical diagnostics, food quality measurement, biological agent detection or environmental monitoring (Lee, 2008).

A biosensor can be defined as a device that sense and converts biological signals to detectable signals. It consists of three main components, namely bioreceptor, transducer and signal processor (Figure 2.1). Bioreceptor is the molecular recognition element which is specific to bioanalytes to be detected. Bioreceptor can be enzyme, antibody/antigen, disease biomarkers, DNA/RNA or microorganisms. They are immobilized onto the sensor surface via physical or chemical interactions. The mostly used forms of bioreceptors used in biosensors are rely on antibody/antigen bindings, DNA/RNA or aptamer interactions, cellular interactions, enzymatic interactions such as microorganisms and synthetic bioreceptor using biomimetic approaches.

In biosensing applications, specific recognition of analyte by bioreceptor is essential. When analyte specifically binds to its bioreceptor, a signal is produced then this signal is converted and read out by a transducer (Kirsch et al., 2013). Transducer type generally identifies the biosensor type. Depending on the signal measuring system, it can be electrochemical, optical, piezoelectric, thermal, acoustic or calorimetric etc. After transducer converts the signal, it is displayed in data processor as quantitatively or qualitatively. (Ali et al., 2017).

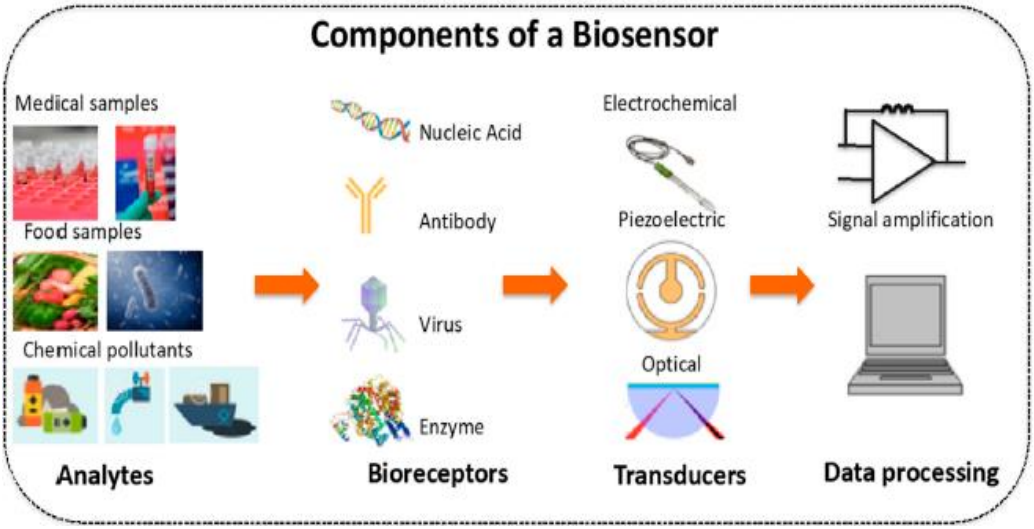

Figure 2.1. Components of a biosensor
(Source: Y. Zhou, Fang, and Ramasamy, 2019)

Biosensors have some characteristics which are used to determine performance of biosensor. These are;

- **Linearity:** It refers the linear relationship between analyte concentration range and biosensor response.
- **Selectivity:** It is the most important characteristic of a biosensor. Selectivity is the ability to specifically recognize only the target analyte in a complex solution. Biosensor should not give a response to any other molecule other than the analyte.
- **Sensitivity:** It is the ability to detect minimum concentration change of an analyte. Minimum concentration that a biosensor detects is defined as limit of detection. It is also related with sensitivity.
- **Stability**: It is the change in sensitivity over time or during long incubation steps.
- **Reproducibility:** It determines the accuracy of a biosensor. A reproducible biosensor gives identical responses in every measurement (Bhalla et al., 2016).

Biosensors have been widely used in various applications. In recent years, biosensors gain importance with the increase in demand for cost-effective, practical, real time systems. In food industry, biosensors are used to monitor food quality and safety such as detection of pathogens or additives. For instance, *Escherichia coli* (E. coli) is a foodborn pathogen and can contaminate vegetables therefore it is crucial to detect E.coli presence in food. In a study, E. coli was detected using potentiometric biosensor systems by indication of pH changes due to ammonium productions (Ercole et al., 2003). Sweeteners are the most common additives in food industry to improve the taste. But excess of sweeteners might cause diabetes, cardiovascular diseases or cancer. For this reason, detection and quantification of sweeteners are important for food safety and consumer health. Biosensors are efficient systems for rapid and low cost detection of sweeteners. Radulescu and coworkers developed an enzymatic biosensor for detection of aspartame which is an artificial sweetener. The proposed biosensor was rapid, low-cost and stable amperometric biosensor (Radulescu et al., 2014). Biosensors were also used for general toxicity detection like heavy metals like lead, copper, cadmium and some kind of pesticides in food safety applications also in environmental safety (Mehrotra, 2016).

Most of the biosensors reported in the last years have been in the category of biomedical applications. They are basically based on molecular recognition mechanisms like antibody-antigen, enzyme-substrate, biomarker-bioreceptor, protein-protein or nucleic acid interactions. In biosensors market today, point-of-care glucose biosensors are widely used especially by diabetic patients for detection of blood glucose levels (Kirsch et al., 2013). These biosensors dominate the biosensors industry with 71.3% market size in 2018 according to Global Market Insight Biosensor Report. Glucose monitoring biosensors have started with Clark and Lyons. With the advancements in science and technology, these biosensors were then improved and categorized as first, second and third generation. Today, commonly used one is the third generation glucose biosensors which is based on sensing of the electrochemical signal produced by electron utilizations in a biointeraction process (Sabu et al., 2019). In the biosensors market, home-use pregnancy tests are also popular biosensors. They are based on detection of human chorionic gonadotropin (hCG) protein which is a pregnancy marker (Gnoth and Johnson, 2014).

Medical biosensors have shown great potential for detection of diseases such as cancer and infectious diseases. Detection mechanism is generally established on molecular recognition of biomarkers of the diseases. Biomarkers include circulating

tumor cells, nucleic acids, peptides or proteins. These biomarkers can be obtained from biological fluids such as blood, urine or saliva. Presence or concentration of biomarkers give information about the stage of the disease. In the last years, antibody-antigen detection systems have been the most extensively developed and applied. For instance, prostate specific antigen (PSA) was used in many studies for detection of prostate cancer. Today, there are devices which give results as fast as 10 minutes noninvasively. Monitoring of carcinoembryonic antigen levels like CA-125, CA19-9 are also possible with biosensors to evaluate the response of a patient to therapy for numerous cancer types (A. Chen and Chatterjee, 2013)(Battersby et al., 2012).

Biosensors for detection of infectious diseases mostly employ antibodies as a recognition agents, In the literature, there are studies about detection of Hepatitis B, dengue, malaria, cholera etc. (Pejcic, Marco, and Parkinson, 2006).

Biosensors are also suitable for drug development studies. This type of biosensors is used to check drug compounds with known bioactivity or to analyze unknown compounds for drug utilization. Antibiotics like penicillin, inhibitors and neuro actives are some of the targets for recent attempts in drug screening biosensors (Keusgen, 2002).

2.2. Types of Biosensors

Biosensors generally classified and named either by their transducer type or bioreceptor type. Biosensors based on bioreceptor types include enzymatic, nucleic-acid based, protein-based. Depending on the transducer types, the most common biosensors are electrochemical, optical, mass-based transducers (Malekzad et al., 2017). Most of electrochemical biosensors relies on amperometry or voltammetry techniques which are related with electrical potentials and current changes in the system. Optical biosensors are based on absorption, scattering or fluorescence phenomenon. In the category of optical biosensors, surface plasmon resonance (SPR) method have been widely reported. SPR occurs through metal nanoparticles such as silver, copper or gold. Biorecognition event in this type of biosensors happens via detection of change in the dielectric constant of the surrounding environment. Mass-based biosensors are usually piezoelectric biosensors which work based on sound vibrations. When binding occurs between receptor

and analyte, the mass change produces vibrations in the piezoelectrical material and this leads to change of the frequency (Vo-Dinh and Cullum, 2000)

2.3. LSPR Theory and Biosensing with LSPR

Surface plasmon resonance (SPR) is an optical phenomenon occurs when polarized light strikes a metal film and excites the conduction band electrons of a metal. These electrons oscillate collectively with a resonance frequency and propagate along the metal surface. As a result, an absorbance peak is produced in the UV-visible range. SPR signal basically originates changes in the local dielectric environment since these changes affect the electron charge density (Willets and Van Duyne, 2007). SPR is highly dependent on size, composition, shape of metals and refractive index of the surrounding. In biosensing applications, SPR technique has been widely used to study the detection of biomolecular interactions. In the past decades, many SPR biosensors have been developed and commercialized since they provide high refractive index sensitivity, label-free and real-time detection. However, fabrication of SPR biosensors is expensive and requires complex instrumentation. Also, SPR only exists in bulk metal and it has large electromagnetic field decay length. Due to these drawbacks, localized surface plasmon resonance (LSPR) has attracted more attention (Kosuda et al., 2011). LSPR exists in metallic nanoparticles (MNPs) and it is highly localized at each individual MNP which enables the design even a single nanoparticle-based biosensor (Figure 2.2). In addition, LSPR can be excited directly when light interacts to the MNP surface without a need for any additional components like prisms. LSPR based biosensors can be easily designed by immobilizing MNPs onto substrates or as a solution of MNPs. Surface of MNPs are functionalized with specific bioreceptors and bioanalytes are detected. LSPR based biosensors require simple laboratory equipment therefore LSPR is a low-cost technique compared to SPR. Especially, while using nanosized particles for sensitive detection, LSPR provides much more favorable system (Mayer and Hafner, 2011).

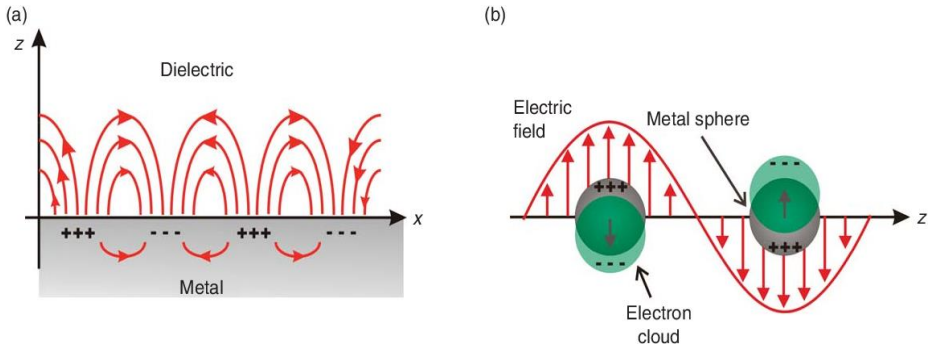

Figure 2.2. Comparison of LSPR and SPR and principle
(Source: Kosuda et al., 2011)

Biosensing with LSPR usually rely on the shift of the peak wavelength in the absorption spectrum. This shift occurs with changes in the refractive index of the environment and it is the indicator of the molecular binding. LSPR shifts can be monitored via a UV-VIS spectrometer.

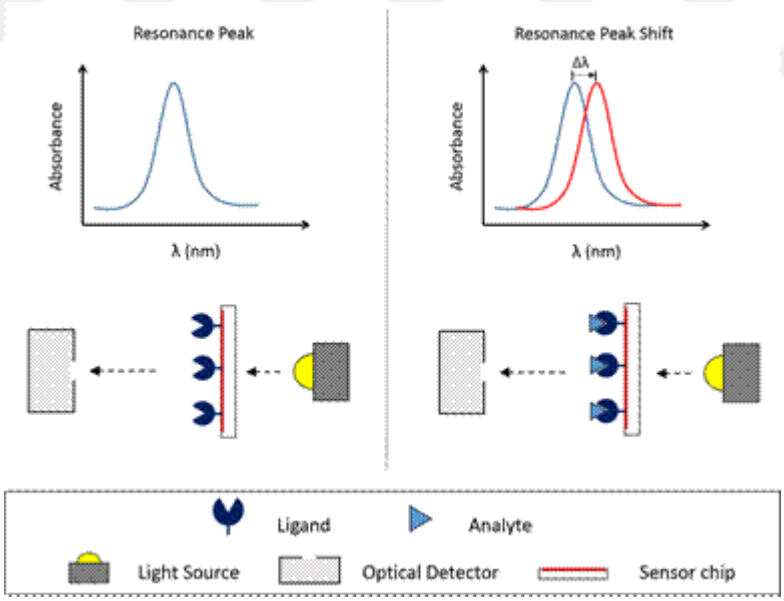

Figure 2.3. Mechanism of detection with an LSPR biosensor
(Source: Nicoya Life, n.d.)

Similar to SPR, peak wavelength of LSPR depends on the composition, size, shape, orientation of the material. Since these properties alter the nanoparticle extinction and scattering, the position and shape of the spectra can vary. Gold and silver are the most common nanomaterials in LSPR biosensing. There are studies reported using these materials in shape of rod, sphere, stars or bipyramids. UV-vis spectra of gold nanoparticles with different shapes is shown in Figure 2.4.

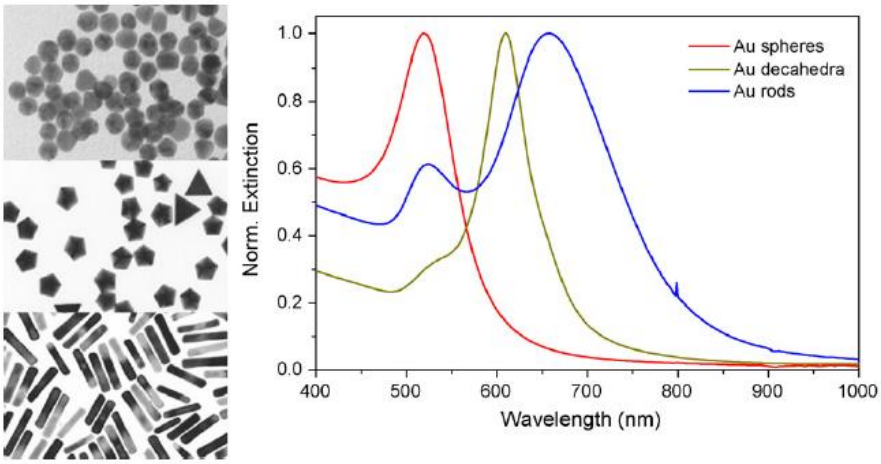

Figure 2.4. Nanoparticle shape effect on LSPR spectra
(Source: Sepúlveda et al., 2009)

2.4. Gold Nanorods in Biosensing

Nanosized gold is one of the most studied noble metals due to its exceptional optical and electrical properties. When compared to other noble metal nanoparticles, gold exhibit strong optical extinction, less toxicity and low reactivity which make them an ideal tool for biomedical applications. Moreover, they have proven to be flexible nanoparticles with facile synthesis and tunability of their size and shape. (Pissuwan, Valenzuela, and Cortie, 2008) In recent years, gold nanoparticles have been used in various shapes including nanorods, nanospheres, nanostars. Among these, gold nanorods have shown great potential for biosensor applications since they provide strong light absorption. (Huang et al., 2007)

Gold nanorods present two absorption bands in absorption spectrum which are longitudinal plasmon band and transverse plasmon band corresponding to long and short axes of electron oscillation, respectively. Transverse plasmon band (TPB) is generally located around 520 nm and it is not sensitive to changes in refractive index of the environment whereas longitudinal plasmon band (LPB) is highly sensitive to changes in the refractive index and occurs at higher wavelength. LPB is dependent on the aspect ratio of GNR. When aspect ratio increases, LPB peak wavelength is red-shifted. It has also shown that LPB is the indicator of molecular binding events on the GNR surface. In biosensing applications, as an analyte binds to bioreceptor on the surface, local refractive index changes and LPB shows a redshift. In terms of sensitivity, shift increases with proportional to concentration of the analyte since it affects the refractive index. (Mannelli and Marco, 2010)

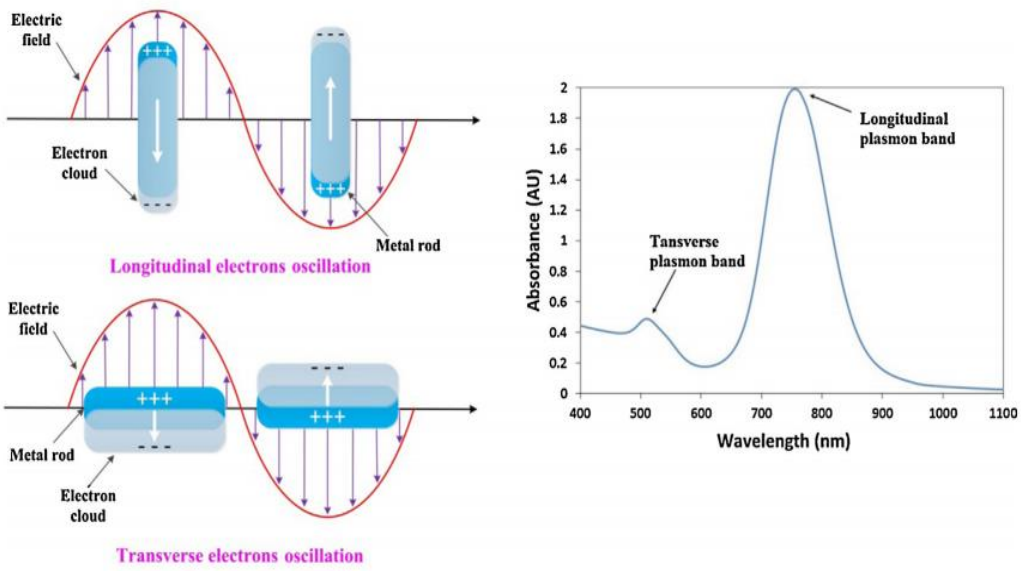

Figure 2.5. Electron oscillations on a gold nanorod surface and LSPR spectra (Source: Cao, Sun, and Grattan, 2014)

2.5. Synthesis of Gold Nanorods

There are two types of synthesis methods to produce gold nanorods: top-down and bottom-up methods. In top-down approach, bulk metal is remodeled to nanoscale size

using different techniques. In bottom-up approach, metal molecules assembly and form the nanoparticles. (Onaciu et al., 2019)

Bottom-up approaches have been the most widely used as they are inexpensive and provide high yield synthesis when compared to top-down approaches. Among bottom-up approaches in the literature, seed-mediated growth method has been the most popular method. This method involves two steps which are preparation of seed solution and growth of this solution to produce gold nanorods. Seed solution is prepared by reduction of gold (III) (Au^{+3}) ions. Thus, seeds which are gold spherical nanoparticles (~4 nm), are produced. In growth solution, these gold seeds are allowed the growth of GNRs in presence of suitable agents. (J. Zhou et al., 2017)

Seed-mediated growth method was first reported by Murphy and coworkers in 2001. They used chloroauric acid ($HAuCl_4$) as the source of gold. In seed solution, $HAuCl_4$ was reduced using sodium borohyride ($NaBH_4$) in the presence of trisodium citrate. After that, seed solution was added to growth solution which was prepared with $HAuCl_4$, cetyltrimethyl ammonium bromide (CTAB) as capping agent, ascorbic acid as weak reducing agent and silver nitrate ($AgNO_3$) for shape and size control (Figure 2.6). However, GNR yield of the final solution was still relatively low. It contained large amounts of spherical shapes as well as the other particle shapes. It was possible to estimate this impurity by comparing the longitudinal and transverse plasmon bands (Jana, Gearheart, and Murphy, 2001). In 2003, El-Sayed et. al. improved this method and minimized the formation of other shapes and increase the yield of the production of gold nanorods. They replaced trisodium citrate with CTAB in the seed solution and they fine-tuned the concentration of silver ions for better controlling of aspect ratio of the gold nanorods. This method provided a high yield as %99 and GNRs with aspect ratios ranging from 1.5 to 4.5 were produced. (Nikoobakht and El-Sayed, 2003)

Seed-mediated method has been optimized in many studies since 2000s and it is still one of the most utilized methods. Since it is a delicate method, parameters like CTAB concentration, reaction time, pH or temperature can alter the size, shape and dispersion of the nanorods. Therefore, while designing the experiments, these parameters should be considered to produce gold nanorods with desired features.

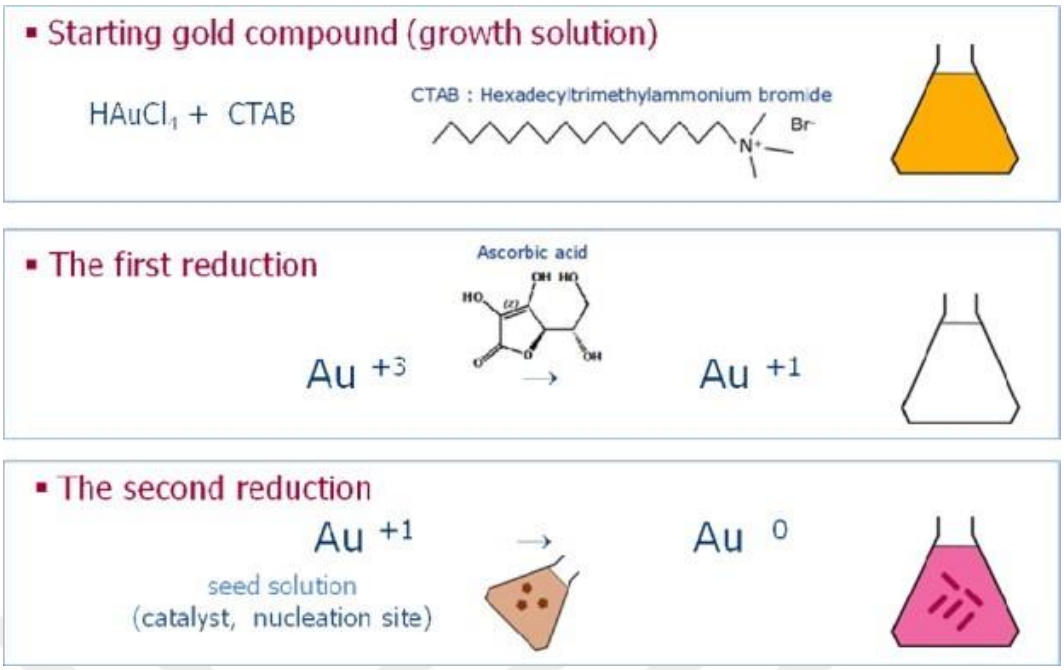

Figure 2.6. Synthesis and reduction steps of GNRs
(Source: Sharma, Park, and Srinivasarao, 2009)

2.6.Surface Modification of Gold Nanorods

CTAB is an essential surfactant for GNR synthesis but it is highly cytotoxic and this restricts the utilization of CTAB-capped nanorods in biomedical applications.(Jia et al., 2020) Moreover, CTAB molecules create a bilayer on the GNR surface and make the surface positively charged. For these reasons, CTAB should be either replaced or covered in order to use GNRs in biological applications. (Nikoobakht and El-Sayed, 2001)

Covering CTAB can be achieved with anionic polyelectrolytes via electrostatic interactions. Polystyrene sulfonate (PSS) and polyacrylic acid (PAA) are well-known anionic polyelectrolytes which have been used for CTAB covering purposes. These molecules can provide attachment of antibodies or other proteins through hydrophobic interactions or covalent bonding such as EDC/NHS chemistry. (Gole and Murphy, 2005)

Additionally, layer by layer (LBL) deposition method have been reported in many studies. Negatively and positively charged polyelectroyltes are successively deposited onto CTAB-capped GNRs. The cycle was repeated multiple times similar to standard

LBL technique. This technique is easy and efficient but due to electrostatic interactions it has stability issue for long time storage. (Huang, Neretina, and El-Sayed, 2009)

Another method for modification of GNR surface is ligand exchange method. The method refers to partially replacement of CTAB with other molecules which provide stability and biocompatibility. In functionalization of GNRs, ligand exchange usually occurs via well-known gold – thiol (SH) bond chemistry due to strong gold – sulfur (S) bond. Thiol terminated polyethylene glycol (PEG) is one of the most commonly used ligands for surface modification of GNRs. (Vigderman, Khanal, and Zubarev, 2012) PEGylated GNRs show high stability in aqueous solutions and some organic solvents. Moreover, they demonstrate low cytotoxicity and high biocompatibility. (Grabinski et al., 2011) In a study, PEG modified GNRs were evaluated in terms of cytotoxicity *in vitro* and stability in physiological conditions. It was shown that PEG is an excellent candidate for replacement of CTAB (Niidome et al., 2006).

2.7. LSPR Based GNR Biosensors

LSPR based GNR biosensors have emerged as powerful tools for detection of biological molecules. They are easy to fabricate, label-free and sensitive systems. Configuration of LSPR based GNR biosensors can be either as suspending GNRs in the solution or immobilizing them on a substrate.

In solution based sensors, surface modification and functionalization also analyte detection are carried out within the GNR solution. Wang et. al. designed a GNR biosensor to detect hepatitis B surface antigen which is related with hepatitis B infection. In the study, after GNR were synthesized CTAB was removed from the GNR surface by centrifugation. Then, hepatitis B surface antibody solution were added to the as-prepared GNR solution directly. The biosensor was qualitatively analyzed in buffer, blood serum and plasma samples. All steps of the experiment took place in the solution. (X. Wang et al., 2010) Compared to substrate based biosensors, solution based biosensors are easy to design. However, solution based GNR biosensors are less stable and aggregates when storaged over a long period of time. Moreover, when GNRs are used in solution form, washing steps after every modification may alter the intensity of the nanorods and lead to inaccurate results. Therefore, immobilizing GNRs on a substrate provide more

controllable and stable biosensor system. (Y. Wang and Tang, 2013) In a recent study, solution based and chip based GNR biosensors were compared with respect to sensitivity and antibody-antigen bindings. Sensitivity of chip based sensor was found to be 297 nm RIU^{-1} while solution based sensor's was only 196 nm RIU^{-1}. Furthermore, chip based sensor had lower limit of detection. (Peixoto, Santos, and Andrade, 2019)

As a substrate, glass is an ideal material since it is optically transparent and cheap. Immobilization of GNRs into glass can be achieved using alkoxysilanes, the reaction is called as silanization. In this reaction, glass surface is initially hydroxylated thus hydrolysable alkoxy groups of silane molecules create covalent bonds with the hydroxyl groups. Afterwards, GNRs are attached to terminal groups of the silane molecules that can be thiol (–SH) or amine ($-NH_2$).

Chilkoti and coworkers fabricated a chip based GNR biosensor as a proof of concept study. Immobilization of GNRs onto glass was acquired by MPTES modification. Firstly, glass substrates were cleaned, then incubated in %10 MPTES solution in ethanol. Next, the substrates were immersed into CTAB free GNR solutions to prepare gold nanorod chips. Mercaptohexadecanoic acid (MHA) and (1-Mercaptoundec-11-yl)tri(ethylene glycol) (EG_3SH) formed a self-assembled monolayer. Following that, streptavidin was conjugated and varying concentrations of biotin was introduced to the surface (Figure 2.7). Detection was carried out via biotin solutions both in PBS and 40% serum. Finally, limit of detection was determined as 94 pM in PBS and 19 nM in serum. They also investigated distance dependence of the LSPR response and found out the sensor could detect refractive index changes up to 40 nm from GNR surface. Moreover, when they compare the results with their previous work on detection with nanospheres, they found out that nanorods based LSPR sensor has much lower detection limit. (Marinakos, Chen, and Chilkoti, 2007).

In another research, GNR based LSPR sensor was developed for detection of circulating antigens of *Schistosoma japonicum* which is a zoonotic infectious agent. After, Indium-Tin-Oxide (ITO) glass slides were cleaned with piranha solution, they were immersed into MPTMS solutions. After overnight incubation, the slides were immersed into as synthesized GNR solutions and GNR chips were prepared for further modifications. Specific antibody was conjugated and antigens were successfully detected in serum samples (He et al., 2017).

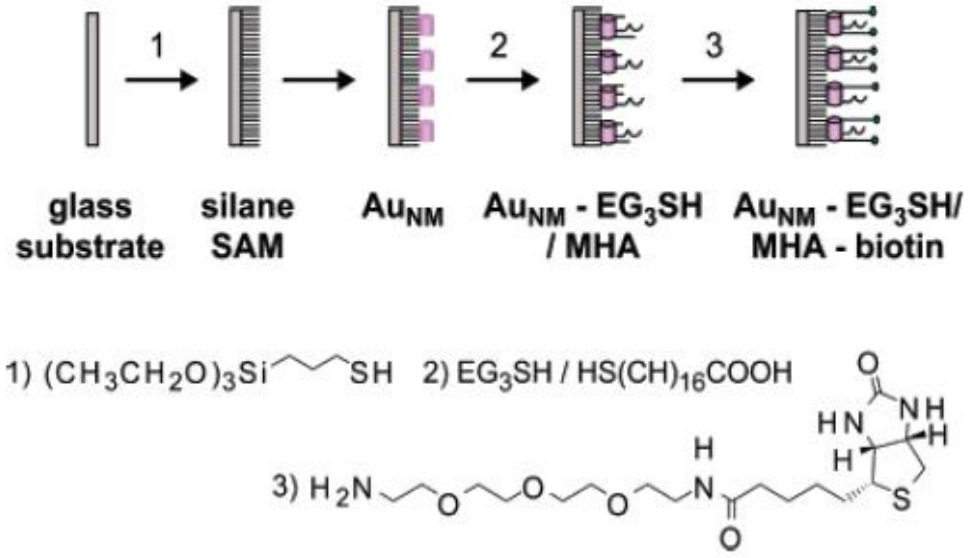

Figure 2.7. Fabrication of the gold nanorod sensor
(Source: Marinakos, Chen, and Chilkoti, 2007)

Balamurgan et. al. investigated shape effect of the gold nanostructures and compared gold nanorods and gold bipyramids by immobilizing both of them onto a glass substrate. The substrate was modified with DNA aptamer which specifically binds to thrombin. The surface was cleaned with piranha solution and submerged into APTES solution in ethanol overnight. Next, glass substrates were incubated in solutions of thiol linked aptamers and (11-Mercaptoundecyl) triethylene glycol (EG_3SH). The response of gold nanorod based biosensors was %25 higher than gold bipyramid based biosensors. (Balamurugan et al., 2013)

2.8. GNR based LSPR Biosensors for Cancer Detection

Cancer is among the leading causes of death in the world today. According to WHO, 18.1 million new cancer cases and 9.6 million deaths were reported in 2018. Worldwide, there are more than 43 million people living with cancer diagnosis for 5

years. In terms of incidence, major cancer types are lung, female breast and colorectal cancers (WHO, 2018).

Cancer is a complex disease arises as a result of genetic or epigenetic alterations. These alterations lead to activation of oncogenes or inactivation of tumor suppressor genes. Currently, diagnosis of cancer is mostly based on invasive techniques such as biopsy. However, this technique is not precise in every case. Besides, detection of early stage cancer may not be possible with invasive techniques. Other techniques like immunoassays can provide more accurate diagnosis but they are time-consuming and costly. Also, they are not sensitive enough for detection of low concentration of cancer markers (Tothill, 2009) , (Soper et al., 2006). Due to these problems, combination of medical biosensors and nanotechnology have been emerged as potential diagnosis tools. Specific biomarkers for particular cancer types are the key element for these biosensors. Biomarkers include tumor associated antigens, altered genes, RNAs, overexpressed proteins, carbohydrates or metabolite molecules. In order to capture these biomarkers, recognition molecules are immobilized onto biosensor surface as a bioreceptor (Nie et al., 2007).

LSPR based GNR biosensors have been used for cancer detection since they are highly sensitive, cost effective and practical. Chen et. al. developed an LSPR based GNR biosensor for detection of breast cancer. Breast cancer marker, cancer antigen 15-3 (CA15-3) was detected by implementing CA15-3 antibody on the GNR surface. In the study, the biosensor was employed to determine CA15-3 levels from breast cancer patient serum samples. In serum samples, CA15-3 concentrations measured by the hospital were compared with the concentrations detected by the biosensor. It was shown that the results were almost the same which confirms the accuracy of the LSPR based GNR biosensor. (S. Chen et al., 2015) In another study, activated leukocyte cell adhesion molecule (ALCAM) cancer biomarker was detected by GNR biosensor. The biosensor was prepared on a glass substrate functionalized with APTES. GNRs were conjugated with ALCAM monoclonal antibody and then recognized the ALCAM antigens. The biosensor yielded 330 nm/RIU sensitivity and a limit of detection as low as 15 pMm (Figure 2.8) (Pai et al., 2017).

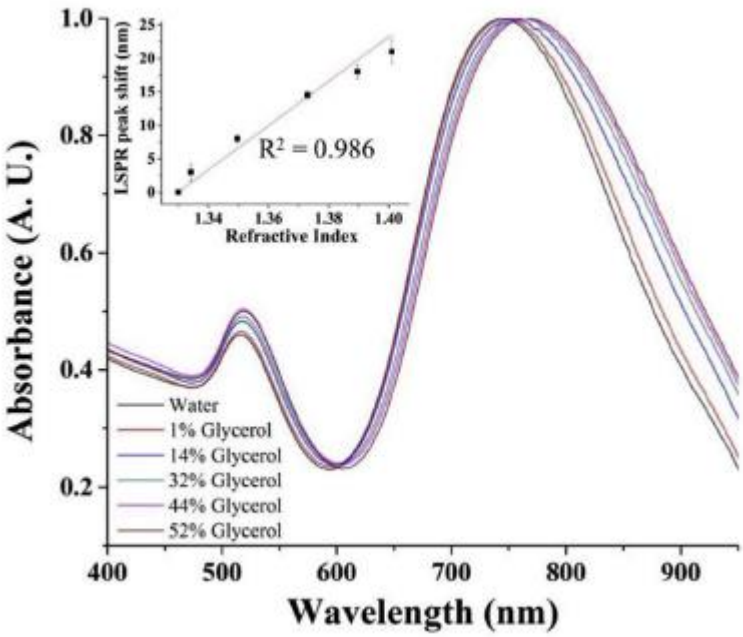

Figure 2.8. Refractive index sensitivity test using solutions with different refractive indexes. Solutions were prepared with varying glycerol contents. Water (n=1.33) was taken as the starting point (Source: Pai et al., 2017).

LSPR based GNR biosensors could detect prostate specific antigen (PSA) which is the most common biomarker for the detection of prostate cancer. GNRs were modified with thiolated oligoethylene (OEG) molecules then immobilized onto MPTES-treated glass slide. After that, antibodies were conjugated onto the surface via EDC/NHS chemistry. Next, PSA antigen was detected with varying concentrations. The lowest concentration detected was 111 aM and 2.79 nm maximum wavelength shift which indicated the biosensor was very sensitive (Figure 2.9). In this study, CTAB-capped GNRs and OEG capped GNRs were immobilized onto the glass slide and their sensor performance were compared. It was concluded that the sensor with OEG-capped GNRs showed higher wavelength shift. (Truong et al., 2011)

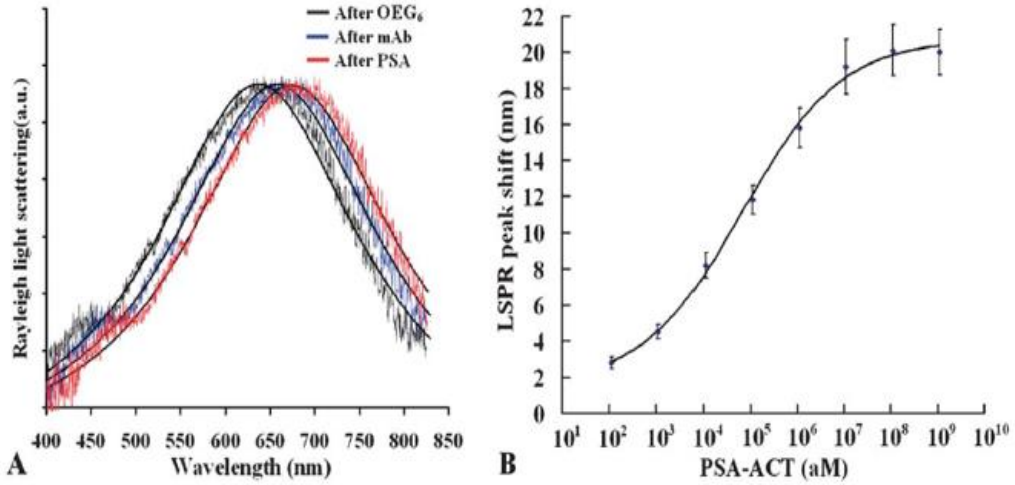

Figure 2.9. LSPR spectra and biosensor response upon detection of prostate cancer biomarker (Source: Truong et al., 2011)

CHAPTER 3

MATERIALS AND METHODS

3.1. Materials

Chemicals: Sodium borohydride ($NaBH_4$), ascorbic acid, silver nitrate ($AgNO_3$), hydrogen tetrachloroaurate(III)hydrate ($HAuCl_4$), hydrogen peroxide (H_2O_2), sulfuric acid (H_2SO_4), N-(3-Dimethylaminopropyl)-N′-ethylcarbodiimide hydrochloride (EDC), phosphate buffered saline tablets (PBS tablets) and silanization molecules were obtained from Sigma Aldrich. Potassium carbonate and Methoxypolyethylene glycol thiol (mPEG-SH) were also purchased from Sigma Aldrich. Hexadecyl trimethyl ammoniumbromide (CTAB) was obtained from Alfa Aesar. Self-assembling molecules (SAM1 and SAM2) were procured from Sigma Aldrich and Santa Cruz Biotechnology, respectively. N-hydroxysulfosuccinimide (Sulfo-NHS) was obtained from Thermo Fisher. DMEM (Dulbecco's Modified Eagle's medium) and Fetal Bovine Serum (FBS) were purchased from Sigma Aldrich. Anti-IgG antibody was procured also from Sigma Aldrich. All the solvents which are ethanol, toluene, methanol were purchased from Sigma Aldrich. Distilled water was obtained from a Millipore Milli-Q Plus water purification system with a 0.22 μm filter. Microscopic slides were acquired from ISOLAB.

Instruments: Attension Theta for contact angle measurements was used. Perkin Elmer UATR Two for FTIR spectroscopy and NanoPlus Particle Sizer and Zeta Potential Analyzer for zeta potential in Biotechnology and Bioengineering Research and Application Centre (BIOMER) at IZTECH were used. For SEM analyzes, FEI Quanta 250 FEG in Materials Research Centre (MAM) at IZTECH was used. Diener Zepto low pressure plasma system for oxygen plasma treatment was used. For centrifuge, Hettich Mikro was used. Localized surface plasmon resonance spectrometer was constructed by connection of Ocean optics USB2000+ spectrometer to an Olympus light microscope.

3.2. Methods

3.2.1. Synthesis of GNRs

Gold nanorods were synthesized in aqueous solution using the seed-mediated growth procedure (Nikoobakht and El-Sayed, 2003). All solutions were prepared with using ultra pure water. Firstly, gold seeds were synthesized by adding 2.5 ml of 0.01 M $HAuCl_4$ solution to 5 ml 0.1 M CTAB solution followed by adding 0.6 ml of 0.01 $NaBH_4$. The solution was vigorously stirred initially and resulted in the formation of a brownish seed solution. Next, the solution was gently stirred for 2 hours. Afterwards, growth solution was prepared with using 0.08 ml seed solution, 20 ml of 0.01 M HAuCl4, 20 ml of 0.1 M CTAB, 0.12 ml of 0.1 M $AgNO_3$ and 0.36 of 0.1 M ascorbic acid. Ascorbic acid was used as a mild reducing agent and changed the growth solution color from brown to colorless. During the synthesis, the color of the solution gradually changed within 15 minutes and finally stabilized. The gold nanorod solutions were grown overnight without stirring at room temperature.

3.2.2. PEGylation of GNR solutions

CTAB on the GNR surface was replaced with thiolated methoxyPEG (mPEG-SH) molecules for immobilization and stabilization on the glass surface. 1 ml CTAB capped GNR solutions were centrifuged twice at 12000 rpm for 15 minutes. After every centrifugation step, supernatants which are CTAB solutions were removed and GNR pellets were dissolved with 1 ml water. Then, potassium carbonate (2 mM) and mPEG-SH (20 mM) were added to every tube and left overnight incubation in dark at room temperature. Next day, solutions were centrifuged at 12000 rpm for 15 minutes to remove free PEG molecules. Supernatants were eliminated and GNR pellets were dissolved again in DI water. PEGylated GNR solutions were collected in a falcon tube. LSPR spectra of the solution were collected.

3.2.3. Development of Biosensor Chips

Two different types of alkoxysilanes (AS1 and AS2) were investigated for silanization of glass surfaces. Firstly, glass surfaces were cleaned with piranha solution (H_2O_2:H_2SO_4 1:3) for 20 minutes. Then, they were extensively rinsed with deionized water and dried under nitrogen flow. Next, the glass chips were separated into two groups to compare the effect of alkoxysilane molecule type on silanization and gold nanorod immobilization. First group was immersed in AS2 solution in acetone for 2 hours. The other was immersed into AS1 solution in ethanol and left overnight incubation at room temperature. After two hours, AS2 treated glass surfaces were rinsed with acetone and dried under nitrogen flow. Then, they were submerged in CTAB-free GNR solution overnight. Next day, these surfaces were rinsed with water and dried under nitrogen. Afterwards, LSPR spectra were acquired. AS1 treated glasses were rinsed with ethanol and deionized water, dried under nitrogen. They were incubated in PEGylated GNR solution overnight. (Mayer et al., 2008) After washing with DI water, they were dried under nitrogen and LSPR spectra were collected.

AS1 treated glass surfaces after GNR immobilization were exposed to low power oxygen plasma treatment for 30 seconds in 200 mTorr to remove the contaminants and mPEG-SH. After obtaining bare GNR surface, sensitivity test was performed to check the response of the chip to increasing refractive index values. Bare GNR coated glass surfaces were immersed into solutions with increasing refractive index values: water (n=1.33), ethanol (n=1.36), ethanol:toluene= 3:1 (n=1.39), ethanol:toluene=1:3 (n=1.43), and toluene (n=1.45), respectively. After immersing the bare GNR coated glass surfaces in each solution, LSPR measurements were carried out. (Marinakos, Chen, and Chilkoti, 2007). Sensitivity test were performed on 5 independent GNR coated glass surfaces.

For functionalization of the GNR coated glass chips, self-assembling molecules with functional groups (SAM1 and SAM2) were utilized. GNR surfaces were conjugated with a mixture of self-assembling molecules at an optimum concentration. The glass chips were immersed in SAMs solution and left overnight incubation. After the surfaces were washed with DI water, they were incubated with EDC (0.4 M) and NHS (0.1 M) in water for 10 minutes. Next, they were exposed to 10 μg/ml antibody in PBS for 2 hours. After antibody incubation, the surfaces were washed several times with PBS and DI water

to remove the unconjugated antibody molecules and other reagents. The antibody conjugation was confirmed via LSPR.

3.2.4. Antigen Detection in PBS and Serum

In biosensor applications, minimizing nonspecific adsorptions is critical. Therefore, before antigen binding studies, the surfaces were incubated in 50 mg/ml BSA in PBS for half an hour. Then, the surfaces were rinsed and incubated with antigen solutions with increasing concentrations in PBS at pH 7.4 for 1 hour. Antigen solutions were prepared at the concentrations ranging from 0.1 nM to 20 μM. To test the GNR biosensor in serum, response of the biosensor in antigen-free complex media were first invesigated. FBS was diluted with cell culture medium at a percentage of %10 or %40. The biosensor chips were incubated in cell culture medium, 10% FBS, %40 FBS or pure FBS. After every incubation, LSPR analysis were carried out. Separately, %40 FBS was spiked with increasing antigen concentrations ranging between 0.1 nM to 20 μM. Antibody immobilized surfaces were incubated in antigen spiked FBS solutions for 1 hour. Then, the surfaces rinsed with PBS followed by LSPR measurements.

Control experiments were carried out to determine the possible non-specific bindings to the biosensor chips prepared. Two different control experiments were performed: In the first experiment, antibody immobilized chip surfaces were introduced with glucose solution (50 mg/ml) in PBS for 1 hour. After 1hour incubation, surfaces were rinsed with PBS and LSPR measurements were carried out. In the second experiment, surfaces were first functionalized with a non-specific antibody, i.e. anti-IgG antibody, following the same method described in Section 3.2.3. The anti-IgG antibody-conjugated surfaces were incubated with 10 μM antigen solution in PBS for 1 hour, then rinsed with PBS and LSPR measurement was taken.

All experiments were carried out in 3 replicates and 5 independent biosensor chips. All LSPR spectra obtained from the experiments were smoothed and normalized with OriginPro 2016 software.

3.2.5. Characterization of the Biosensor

3.2.5.1. Water Contact Angle Measurement

Contact angle measurement was performed to determine wettability of the surfaces. Measurements were carried out with silanized surfaces.

3.2.5.2. Scanning Electron Microscopy (SEM)

SEM images were obtained with FEI Quanta 250 FEG microscope under 2 kV. Size and distribution of the gold nanorods were analyzed.

3.2.5.3. Fourier Transform Infrared (FTIR) Spectroscopy

Perkin Elmer UATR Two instrument was used to characterize the molecules on the surface before and after modifications. The measurements were carried out before and after oxygen plasma treatment and also on SAM formed surfaces.

3.2.5.4. Zeta Potential Measurement

Zeta potential of the surfaces was measured with Nanoplus Particle Sizer instrument. Laser source was diode laser with a wavelength of 660 nm. Measurements were took place -500 mV to +500 mV. Measurements were carried out in PBS 7.4 and distilled water.

CHAPTER 4

RESULTS AND DISCUSSION

4.1. GNR Synthesis and PEGylation

Gold nanorods were successfully synthesized by seed-mediated growth method. CTAB was used as a surfactant and stabilizer. Firstly, seed solution was prepared by using $HAuCl_4$ as gold source. Then, the gold seeds in this solution were allowed to grow into nanorod shape using a growth solution. In the growth solution, $AgNO_3$ was used to adjust the size of the gold nanorods also increase the yield. Figure 4.12 shows the LSPR spectra of the synthesized GNRs. The spectra show that the transverse plasmon peak wavelength was at around 520 nm and the longitudinal plasmon peak wavelength was at 675 nm. For gold nanorods, the transverse plasmon band is generally between 500-550 nm and it is related with the diameter of GNRs. Therefore, the transverse plasmon band of the synthesized gold nanorods were consistent with the literature. Longitudinal plasmon band (LPB) is proportional to the aspect ratio of GNRs. The relationship between longitudinal plasmon band and the aspect ratio is shown with the following formula (Yan, Yang, and Wang, 2003):

$$\lambda_{max} = 95R + 420 \text{ (Equation 1)}$$

where R is the aspect ratio. From this equation, the aspect ratio of GNRs synthesized in this study was found to be ~2.68. The synthesized gold nanorods kept their stability in solution form for 6 months. This long term colloidal stability was provided by CTAB. But, to be able to use GNRs in biosensing applications it is crucial to eliminate CTAB and using GNR solution freshly for modification steps.

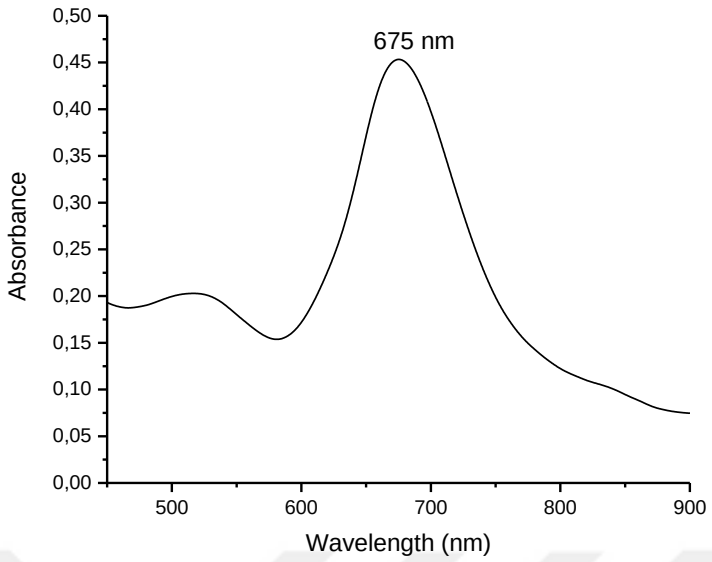

Figure 4.1. LSPR spectra of synthesized GNRs

In biomedical applications, utilization of CTAB capped GNRs are not favorable due to high cytotoxicity of CTAB. Additionally, CTAB creates cationic bilayer on GNR surface which adversely affects further functionalization steps and causes non-specific interactions with serum proteins. However, complete CTAB removal leads to aggregation of GNRs since CTAB provides great stability to gold nanorods. To displace CTAB and maintain stability, a thiol terminated PEG was used as a stabilizer. Exchange of CTAB with PEG took place via strong gold-thiol bond. In this study, CTAB was decanted by two steps centrifugation and then GNRs were modified with mPEG-SH. The binding of thiolated PEG led to red-shift on λ_{max} of longitudinal plasmon band (Figure 4.2). A red-shift of 3 nm was observed on LSPR spectra which indicated CTAB was successfully exchanged with PEG. This shift on maximum absorption wavelength can be attributed to change on the refractive index on the GNR surface.

PEG provides uniformity when GNRs are deposited onto glass slides. Therefore, it prevents aggregation and prepares the GNR coated surface for further modifications. (Mayer et al., 2008)

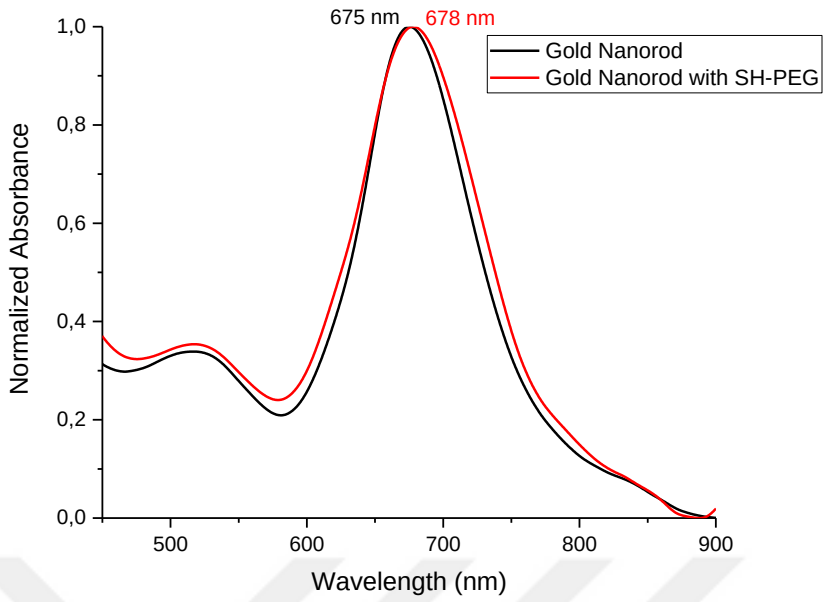

Figure 4.2. LSPR spectra of GNR before and after PEGylation

4.2. Preparation and Characterization of GNR Coated Glass Surfaces

Biosensor chips were prepared on microscopic glass slides. Firstly, piranha solution was prepared for cleaning slides to eliminate organic residues and contaminants. This solution is a mixture of sulfuric acid and hydrogen peroxide and it hydroxylates the surface. This hydroxylation is important for further modification of the surface with silane molecules. Silane molecules react with the –OH groups on the surface and form Si-O-Si bonds. In this study, two types of organosilanes, coded as AS1 and AS2 were compared,. After both modifications, surfaces were expected to be hydrophobic. Contact angle measurements were done to determine wettability of the surfaces (n=3). AS1 modified surfaces showed 69° contact angle of water, whereas, AS2 modified surfaces showed 10° contact angle of water (Figure 4.3). This result indicated that AS1 was successfully bound onto the surface while AS2 did not.

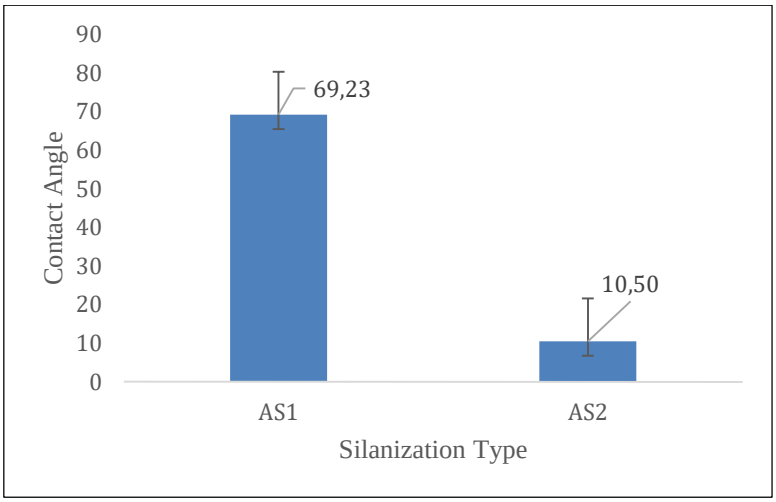

Figure 4.3. Water contact angle comparison of surfaces modified with different alkoxysilane molecules (AS1 and AS2)

Immobilization of GNRs onto both types of silane modified surfaces were also compared. After washing and drying steps, SEM characterizations were carried out. Figure 4.4 displays SEM images of both surfaces. GNRs on AS1 modified surface were homogenously distributed on the surface, there was no aggregation, whereas GNRs on AS2 modified surface tended to aggregate. After these analyses, the best GNR distrubition was found to be on AS1 modified surfaces. Thus AS1 was chosen as a silanization agent for GNR coating and further functionalization steps.

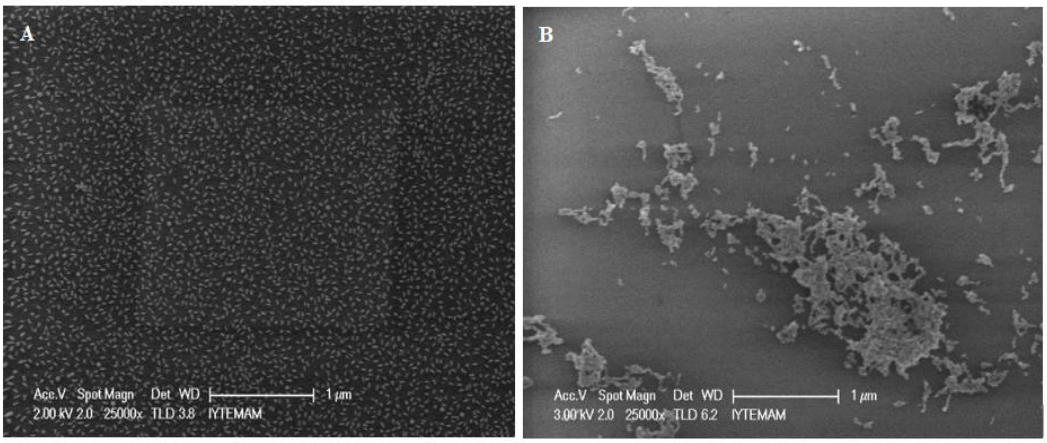

Figure 4.4. SEM images of AS1 (A) and AS2 (B) modified and GNR coated glass surfaces

GNR coated surfaces were developed with immersing AS1 modified surfaces into PEGylated GNR solutions overnight. It was possible to determine successful GNR coating from the blueish color of the glass surfaces (Figure 4.5). Next, the surfaces were exposed to oxygen plasma treatment to obtain a bare gold surface. Oxygen plasma removed PEG and other contaminants. Oxygen plasma does not affect AS1 bonds thus it did not have an effect on attachment of gold nanorods on the surface. After coverage of the surface with GNRs, blue shift was observed on the maximum peak wavelength comparing to the solution form of GNRs (Figure 4.6). This blue shift was attributed to the removal of PEG layer with oxygen plasma treatment and arrangement of GNRs on the surface. Another cause of this situation was thought to be side to side coupling of nanorods which could lead to blue shift on the peak wavelength (Tan, Anand, and Mirsaidov, 2017). Immobilized GNRs exhibited an LSPR peak wavelength of 670 nm.

Figure 4.5. Before and after immobilization of GNRs onto glass substrates

SEM images of oxygen plasma treated GNR coated glass surfaces showed that GNRs were homogeneously distributed on the surface and there was no aggregation (Figure 4.7). Images also confirms that oxygen plasma treatment did not affect GNR deposition or any linkages between the molecules. As seen from the Figure 4.7 size of the nanorods were approximately 40-50 nm which was consistent with the LSPR results. In the SEM images, GNRs were seen parallel to the surface which was expected since they tend to adsorb onto the surface with a maximum contact area. (Marinakos, Chen, and Chilkoti, 2007)

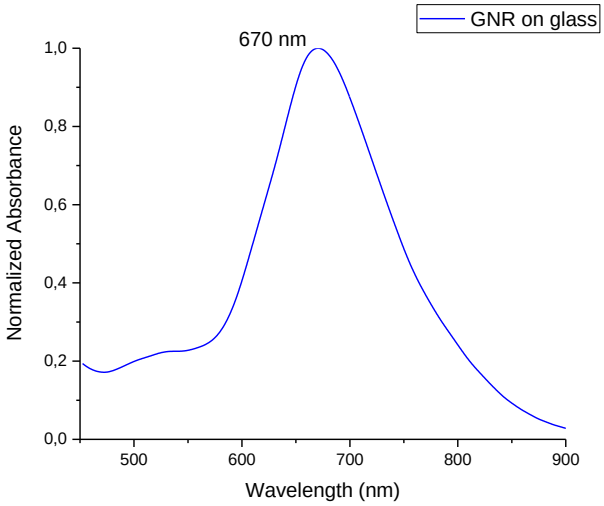

Figure 4.6. LSPR spectra of GNRs after immobilization on a glass surface

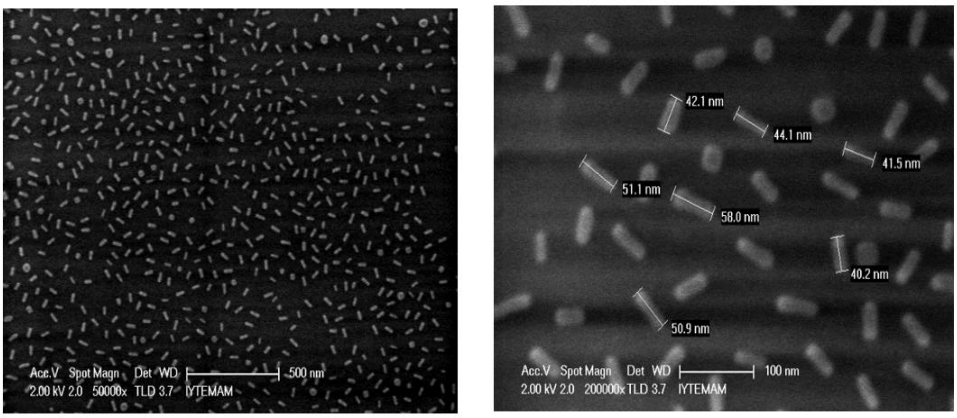

Figure 4.7. SEM images of GNR coated surface after oxygen plasma

4.3. Sensitivity of GNR Coated Glass Surfaces

Biosensing with LSPR is based on detecting peak wavelength shift with respect to the change in refractive index of the medium and this change is related with sensitivity. The sensitivity of LSPR biosensors is generally referred in nm/RIU which means LSPR peak wavelength per unit of refractive index change. In other words, this value defines how the biosensor response to difference in local dielectric environment. (Liao, Nehl, and Hafner, 2006)

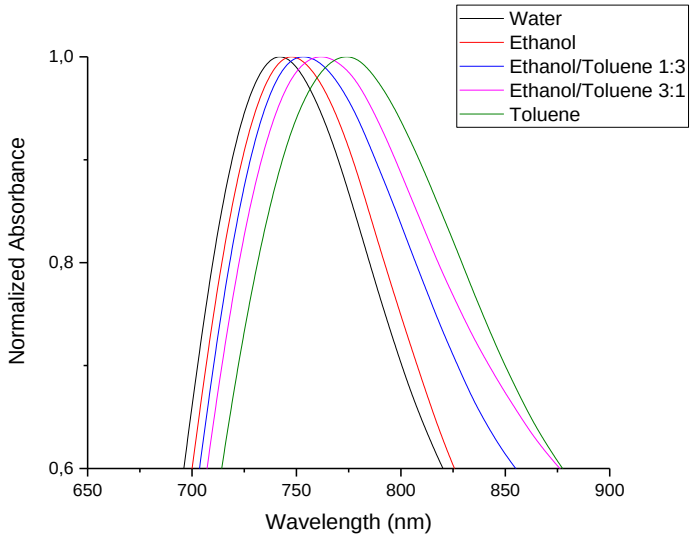

Figure 4.8. Refractive Index Sensitivity on LSPR spectra

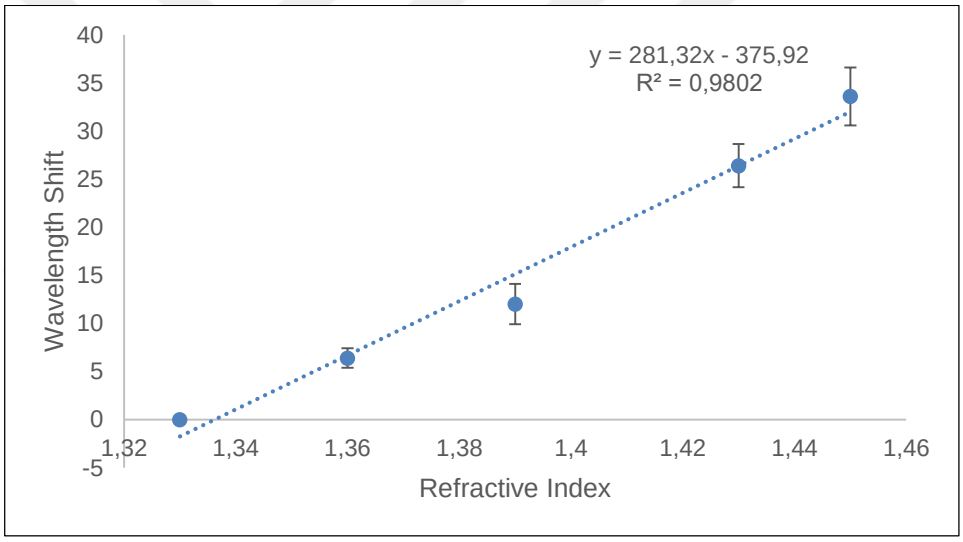

Figure 4.9. Refractive index versus wavelength shift plot

In this study, sensitivity of the biosensor was investigated by immersing glass chips into solutions with increasing refractive indexes. LSPR spectra were collected for each solution. The results are shown in Figure 4.8. As expected, when refractive index of the solution increased, peak wavelength red shifted. The change of the refractive index versus wavelength shift was plotted and a linear relationship was achieved. (Figure 4.9) The slope of this plot indicates the sensitivity and it was found to be as 281 nm/RIU (n=5). This result was compared to LSPR based biosensors designed with different nanoparticles

such as gold nanospheres (Underwood and Mulvaney, 1994) , gold nanostars (Nehl, Liao, and Hafner, 2006) and gold nanorods with similar aspect ratio (Truong et al., 2011). It can be concluded that the developed GNR biosensor is highly sensitive.

4.4. Modification of GNR Coated Glass Surface

High yield detection on GNR biosensors could be achieved only when the surface is functionalized with the appropriate molecules. It is crucial to prevent nonspecific bindings and to functionalize the surface for optimal antibody-antigen interaction.

In the thesis, a mixture of self-assembling molecules with functional groups was prepared. Figure 4.10 demonstrates that when self-assembling molecules adhered at the surface, 23 nm λ_{max} red-shift occurred since refractive index of the surroundings was changed.

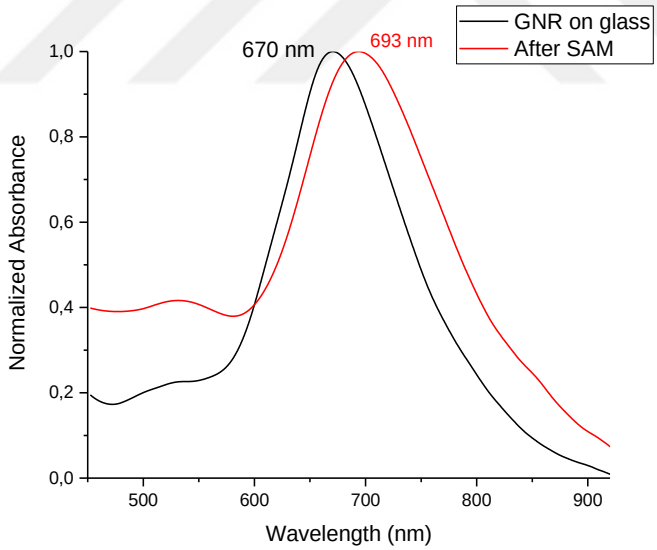

Figure 4.10. Binding of SAMs on LSPR spectra

Functionalization of the surface was also confirmed with FTIR and zeta potential measurements. Figure 4.11 shows FTIR data obtained from PEGylated GNR surface, bare GNR surface and SAM formation on the surface. Before oxygen plasma treatment, there

were PEG chains on the surface (shown in red). Peaks at around 897 cm^{-1} and 1073 cm^{-1} be attributed to CH_2 rocking and stretching of C-O-C in ethylene glycol moieties, respectively (Seol et al., 2013). Peak of the bare gold surface did not show any significant peak which is consistent with the literature (Ermiş, Uzun, and Denizli, 2017)·(Singh, Verma, and Arora, 2014). After SAM formation, strong peaks were observed in the spectrum in accord with the chemical structure of self-assembling molecules. Peaks at around 3700 cm^{-1} is corresponding to –OH stretch. The strong bands in the CH-stretching region at around 2900 cm-^{1} indicates the symmetric –CH_2 stretching on SAMs. The strong peaks at between 1142 cm^{-1} and 1385 cm^{-1} can be assigned to CH_2 – CH_2 wagging and CH_2 scissoring and CH_2 twist modes. Around 1385 cm^{-1} and 1742 cm^{1}, significant –COOH moieties were observed. (Harder et al., 1998)

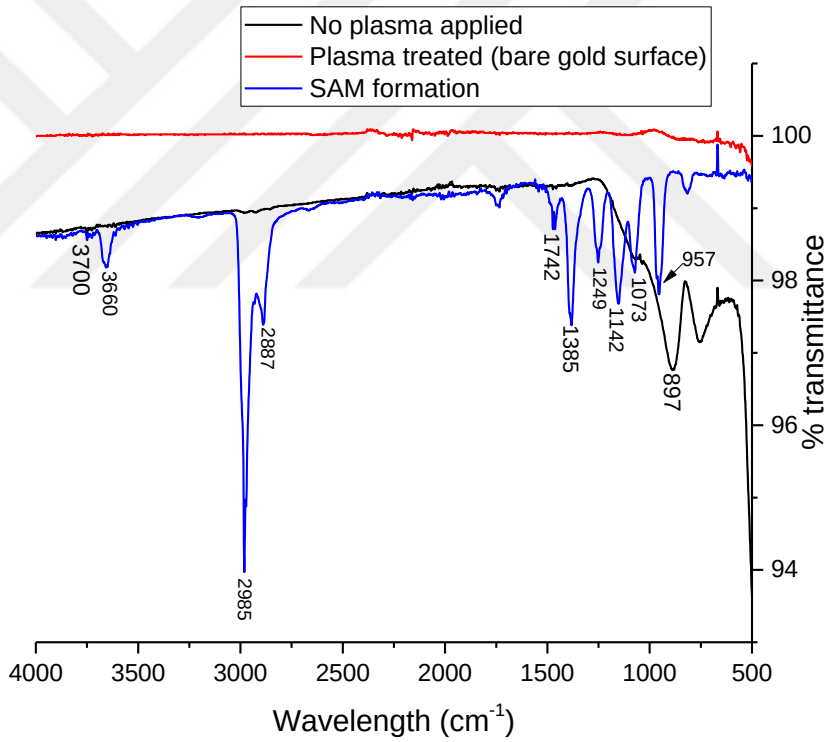

Figure 4.11. FTIR spectrum of plasma treated, no plasma applied and plasma treated-SAM formed surfaces

Immobilization of antibody took place via EDC/NHS chemistry. –COOH group of SAMs reacts with EDC and forms an amine reactive intermediate. Sulfo-NHS converts

this intermediate to NHS-ester and creates a stable amide bond between carboxylic acid of the surface and amine group of the antibody (Bart et al., 2009). After two hours of incubation in antibody solution, surfaces were rinsed and LSPR spectra was collected. A representative 6 nm red-shift occurred which indicated successful antibody binding on the surface. (Figure 4.12)

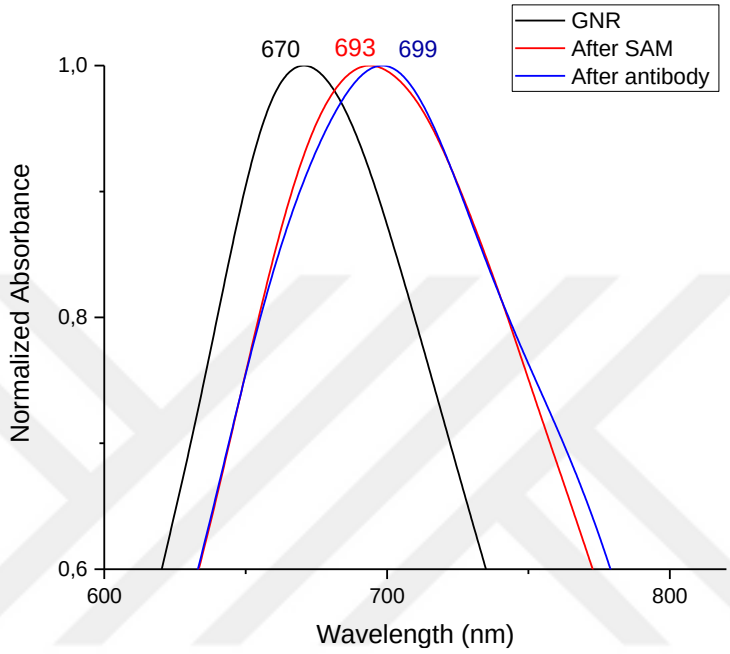

Figure 4.12. Antibody binding on LSPR spectra

Also, zeta potentials after antibody immobilization were measured and the results are shown in Table 1. Initially, zeta potentials of synthesized CTAB capped GNRs and PEGylated GNR solutions were determined. PEGylation of GNR resulted in a decreased surface charge from +63.24 mV to -4.87 mV. Since CTAB is a net positively charged molecule, ligand exchange between CTAB and PEG led to this decreasing in agreement with the literature. (Vonnemann et al., 2014) Zeta potential of the antibody in PBS was found as -5.27 mV. On the surface, before and after plasma treatment results showed that removal of PEG from the surface caused increased of zeta potential from -10 mV to +3.85 mV. After the adsorption of self-assembling molecules on the surface, zeta potential turned to negative. This is because negative charges arising from –COOH groups. When antibody was bound onto the surface, negative charge increased from -0.83 to -3.08 as expected.

Table 1. Zeta potential measurements

	Sample Type	Zeta Potential (mV)
Solution	CTAB capped GNRs	+63.24 ± 6.1
	PEGylated GNRs	-4.87 ± 2.4
	Antibody in PBS 7.4	-5.27 ± 1
Glass Surface	No oxygen plasma applied (PEGylated GNR coated surface)	-10.05 ± 0.4
	Oxygen plasma applied (bare gold surface)	+3.85 ± 0.7
	Plasma treated SAM Formed Surface	-0.83 ± 0.1
	Plasma treated-SAM formed-Antibody Conjugated Surface	-3.08 ± 1.8

Effect of self-assembling molecules on nonspecific bindings, was investigated with incubation of the bare GNR surface in antibody solution. On a separate surface, SAM molecules were formed on the surface without performing the subsequent EDC/NHS chemistry. The surface was then incubated within specific antibody solution. LSPR measurements of both surfaces were compared. When antibody was incorporated to bare gold surface, an obvious shift occurred in LSPR spectra. This red-shift was assigned to non-specific binding of gold nanorods to amine groups of the antibody. Amine-gold bond is much weaker bond than thiol-gold bond and can be considered similar to noncovalent bonds in terms of bond strength (Hoft et al., 2007). Also, amine-gold bond may cause aggregation problems. Therefore, functionalization of the surface with self-assembling molecules is important. When self-assembling molecules were present on the surface, they prevented nonspecific bindings by means of the protein repelling nature of the functional groups on self-assembling molecules. No shift was observed even at 50 µg/ml

antibody concentration. It can be concluded that SAM molecules are capable of preventing nonspecific bindings. (Figure 4.13)

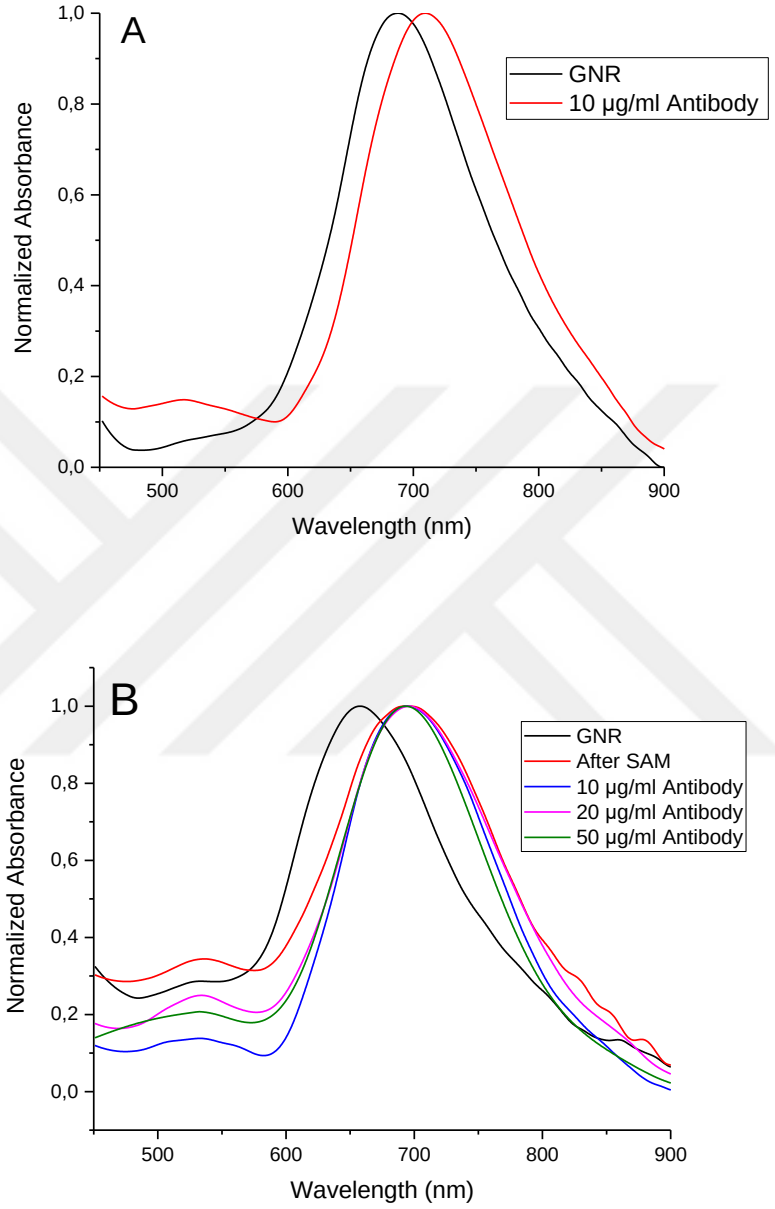

Figure 4.13. Effect of self-assembling molecules on preventing nonspecific bindings A) Antibody incubation without SAM and EDC/NHS B) Antibody incubation after SAM formation without EDC/NHS.

4.5. Control Experiments for Determination of Selectivity and Specificity

Selectivity is one of the most important characteristic of a biosensor. A good biosensor should respond to only specific target molecules. Evaluation of selectivity of proposed GNR biosensor was carried out with glucose and BSA at higher concentrations than antigen concentration at the saturation point. Glucose was chosen for the reason that it is a small saccharide molecule like the biomarker to be detected. Therefore, comparison of the responses of the biosensor to glucose and the antigen is significant. Figure 4.14 illustrates LSPR spectra when antibody coupled surface was incorporated with glucose, BSA and the antigen, respectively. It was found that GNR biosensor did not respond to any molecule other than its specific target. Based on this result, selectivity of the biosensor was confirmed.

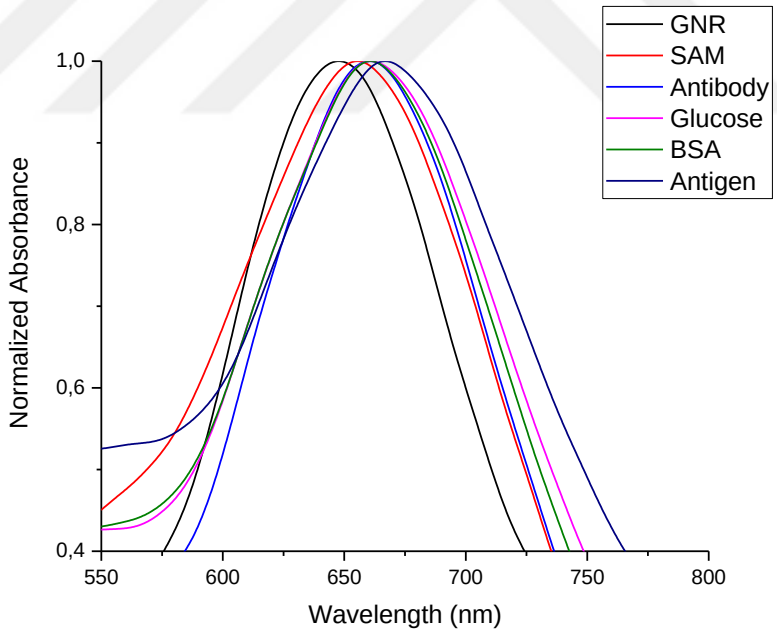

Figure 4.14. Specificity of the antibody to the antigen on LSPR spectra

After selectivity test, specificity of the biomarker to its antibody was investigated. An anti-IgG antibody was used for this purpose. Anti-IgG antibody conjugated surface

was incubated with the target sialic acid solution at the highest concentration tested (10 μM). LSPR spectra indicated that the target analyte did not bind to anti-IgG antibody functionalized surface which proves that the developed GNR biosensor was specific and selective. (Figure 4.15)

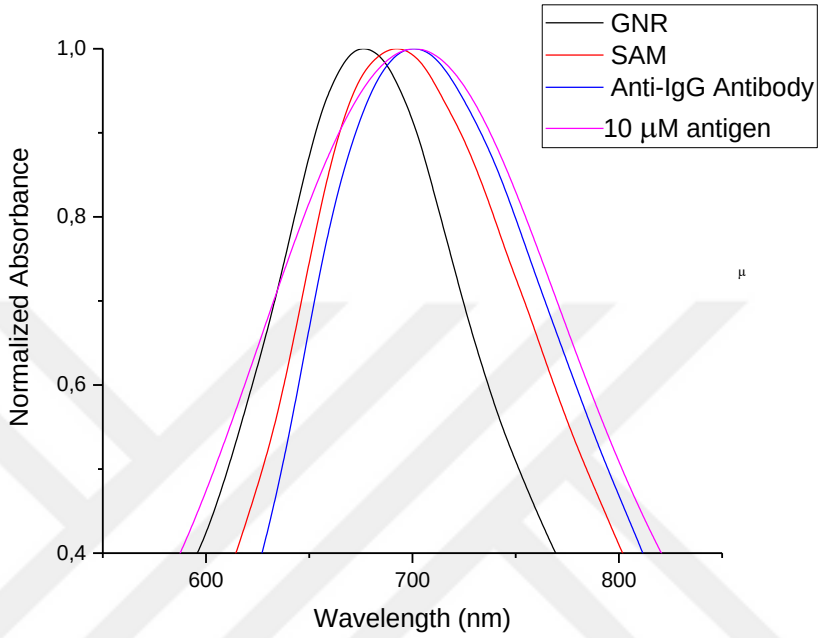

Figure 4.15. Antigen incorporation onto surface modified with non-specific anti-IgG antibody. Antigen did not bind and no shift was observed on LSPR spectra.

4.6. Antigen Detection in PBS and Serum

After antibody immobilization, GNR biosensor chips were treated with BSA solution to minimize nonspecific bindings during antigen detection experiments. BSA is a well-known blocking agent since it successfully blocks remaining non-functional spaces on the surface. (Ahirwar et al., 2015) Next, GNR biosensor chips were incubated in different solutions (serum or PBS pH 7.4) with increasing antigen concentrations. Before checking detection ability of GNR biosensor in serum, a control experiment was performed to determine the non-specific binding effect of serum solutions. In this control experiment, the biosensor chip was first interacted with cell culture media (DMEM)

having varying serum contents. Glass chips were immersed in cell culture medium having increasing FBS concentrations. Except 100% FBS, no red-shift was observed on LSPR spectra (Figure 4.16). A 2 nm red-shift for 100% FBS was attributed to the non-specific binding events due to the high protein content of the serum. Serum is a complex medium and when the biosensor chip was exposed to serum, nonspecific adsorption of various proteins may occur. (X. Wang et al., 2010) To eliminate this signal distortion for measurements, 40% FBS concentration was selected for spiking the serum solutions with the target antigen for detection experiments to be performed with serum samples.

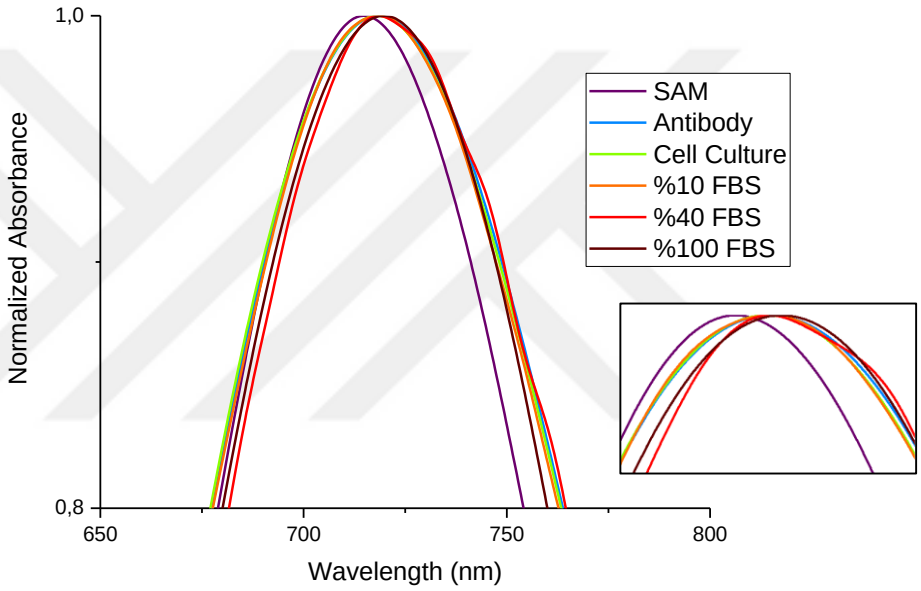

Figure 4.16. Response of the biosensor chip in different complex media. Chip surface after: SAM modification (purple); specific antibody conjugation (blue); treatment with cell culture medium without serum (green); treatment with cell culture medium with 10% (orange), 40% (dark orange), 100% (black) FBS.

Antigen detection experiment was carried out both in PBS 7.4 and cell culture medium containing %40 FBS. First, antigen concentrations were adjusted ranging between 0.1 nM – 20 μM by spiking the relevant solution with antigen solution to yield the desired final antigen concentration. Figure 4.17 illustrates the LSPR spectra and λ_{max} shifts versus varying antigen concentrations in PBS. At the lowest applied concentration

which is 0.1 nM, there was not any detectable shift. As the antigen concentration increased between 1 nM and 10 µM, λ_{max} red-shifted in a detectable manner as a consequence of antigen binding and change of the refractive index. Maximum λ_{max} shift was determined approximately 12 nm at 10 µM. (Figure 4.18) The curve demonstrates a sigmoidal fit which is consistent with the literature.(Truong et al., 2011),(Truong, Kim, and Sim, 2012),(Kim et al., 2009),(Gobi, Kataoka, and Miura, 2005) This sigmoidal shape indicates the upper and lower working limits of the biosensor within the plotted region. Like most of label free biosensors, the surface tends to saturate at some point (Lavín et al., 2018). The sigmoidal curve obtained from 5 independent measurements for every concentration was indicative of the saturation point at 10 µM.

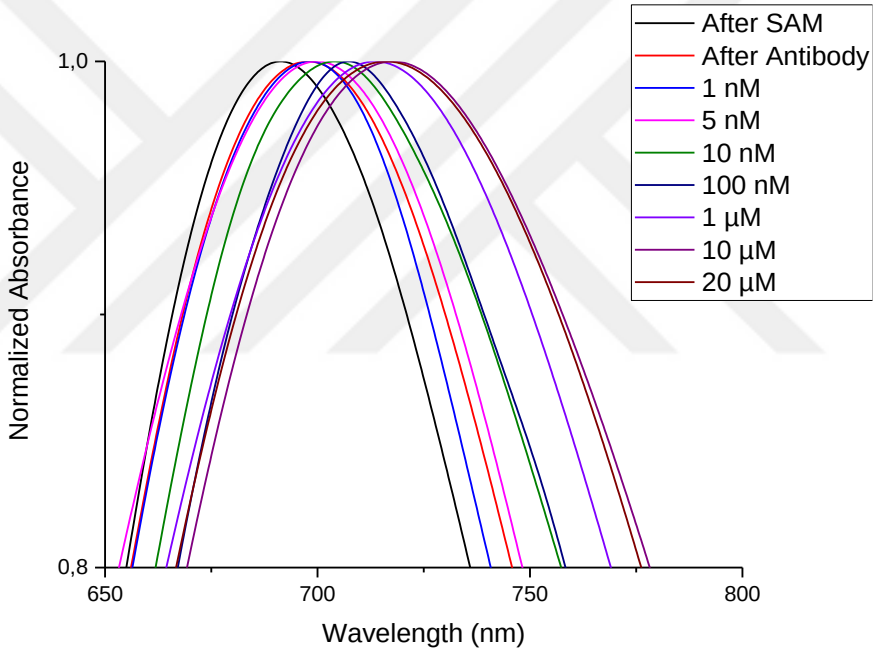

Figure 4.17. LSPR spectra of specific antibody functionalized biosensor chips after treatment with PBS solutions having varying antigen concentrations

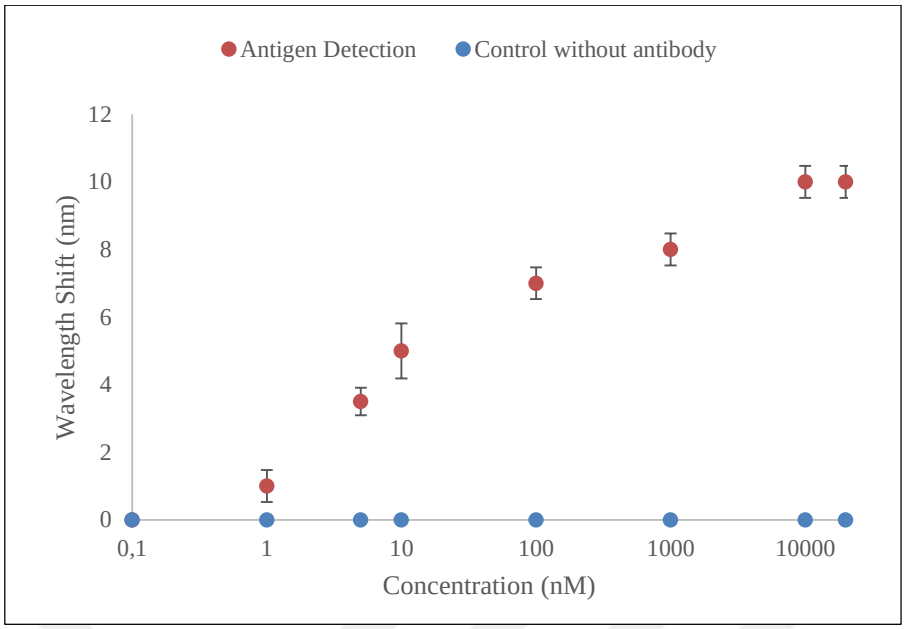

Figure 4.18. Antigen concentrations versus LSPR peak wavelength shifts determined for specific antibody functionalized biosensor chips after treatment with PBS solutions having varying antigen concentrations. The error bars represent standard deviation for measurements of 5 independent biosensor chips (n=5)

The biosensor chips were also tested with cell culture medium containing 40% FBS and increasing antigen concentrations. In Figure 4.19, LSPR λ_{max} shifts for varying antigen concentrations are shown. Unlike the PBS measurements, there was not any detectable shift for 1 nM and 5 nM antigen concentrations. Lack of bindings at these low concentrations can be related with high complexity and protein content of serum. High protein content could dominate the very low analyte concentration or create biofouling on the nanorod surface (Unser et al., 2015). Moreover, serum proteins could affect sensing distance of the biosensor.(Marinakos, Chen, and Chilkoti, 2007) Antigen recognition was found to start from 10 nM and reached to saturation at 10 µM which was in accord with PBS results. Similar to PBS results, wavelength shift versus concentration curve displayed sigmoidal shape. (Figure 4.20) For both PBS and FBS measurements, shifts were similar. Antigen detections in both FBS and PBS are statistically significant. ($p<0.05$)

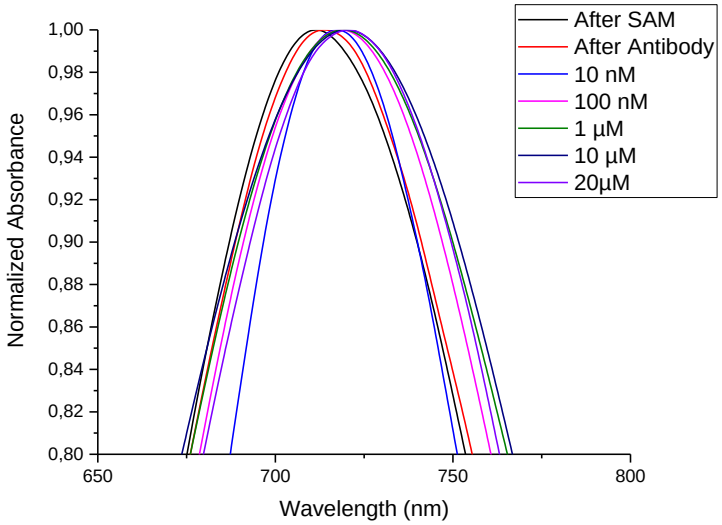

Figure 4.19. LSPR spectra of specific antibody functionalized biosensor chips after treatment with cell culture media having varying antigen concentrations

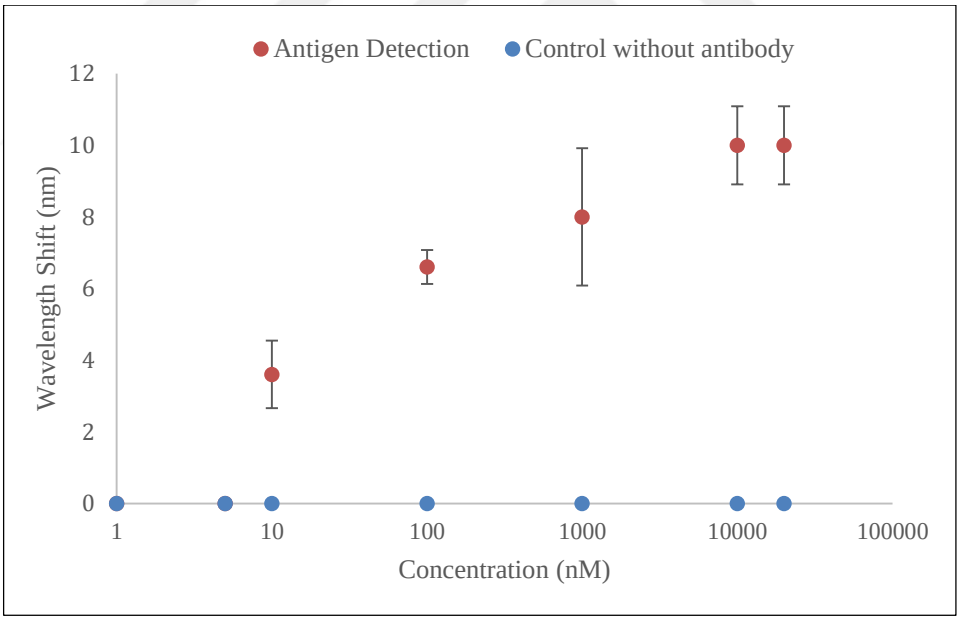

Figure 4.20. Antigen concentrations versus LSPR peak wavelength shifts determined for specific antibody functionalized biosensor chips after treatment with cell culture media having varying antigen concentrations. The error bars represent standard deviation for measurements of 5 independent biosensor chips (n=5)

CHAPTER 5

CONCLUSION

The aim of this thesis is to develop a label-free, sensitive and specific LSPR based biosensor against a potential cancer biomarker by using optical properties of gold nanorods. The biosensor was fabricated by immobilizing GNRs onto glass slides and functionalizing the surface with the appropriate molecules. In this study, the analyte is a sialic acid which is a potential cancer biomarker. Specific monoclonal antibodies against this analyte was conjugated onto the surface and detection was carried out in PBS and cell culture medium containing serum. Molecular bindings were monitored with the shift of maximum peak wavelength on the LSPR spectra.

GNRs have exceptional optical properties which make them ideal materials for utilization in biosensors. They have high sensitivity to refractive index change of the surrounding. Herein, this high refractive index sensitivity of GNRs was used as an essential feature for the detection. Firstly, CTAB stabilized GNRs were synthesized at around 40-50 nm and with the aspect ratio of ~2.7. In LSPR spectra, transverse plasmon peak was at around 520 nm and longitudinal plasmon peak was around 675 nm. The GNRs were PEGylated with mPEG-SH molecules to replace CTAB on the GNR surface and to maintain the stability of the GNRs. This ligand exchange was observed on LSPR spectra as 3 nm shift on the maximum peak wavelength. For immobilization of the PEGylated GNRs on the glass surface, glass surfaces were modified with silane molecules. After activation of –OH groups on the surfaces, they were modified with different silane molecules and characterized with contact angle measurements. The refractive index sensitivity of silanized GNR coated surfaces was found to be as 281 nm/RIU. After GNRs were immobilized onto glass surfaces, they were modified with self-assembling molecules with functional end groups. These molecules enabled antibody conjugation via EDC/NHS chemistry and also played role in preventing nonspecific bindings. Binding of self-assembling molecules on the surface was confirmed with a 23 nm red-shift of the maximum peak wavelength on the LSPR spectra. In zeta potential analysis, it was shown that self-assembling molecules attachment reduced the surface charge because of the negative charges on carboxylic acid moieties. FTIR analysis also

confirmed the successful binding of self assembling molecules onto the surface. Furthermore, Functionalized surfaces did not show any binding of antibody without EDC/NHS whereas the surface without self assembling molecules showed an obvious red-shift in the LSPR spectrum indicating non-specific binding.

Analyte specific antibody was conjugated onto the surface via EDC/NHS chemistry. Maximum peak wavelength on LSPR spectra red-shifted 6 nm after antibody conjugation which indicated the successful conjugation of antibody. Results of zeta potential measurements also confirmed that the antibody was conjugated onto the surface. Control experiments were carried out by exposing the biosensor chips to molecules other than the target analyte. It was shown that the developed biosensor only responded to the target analyte which proved the specificity of the biosensor.

After the GNR biosensor surfaces were developed, antigen detection experiments were performed in PBS 7.4 and cell culture medium containing 40% FBS. The solutions were spiked with varying concentration of antigens and then exposed to biosensor chips. . Limit of detection in PBS was found to be 1 nM. Sigmoidal shape of the wavelength shift vs. antigen concentration curve indicated that the biosensor chips were saturated at 10 μM antigen concentration which is consistent with the relevant literature. Limit of detection in serum containing culture medium was 10 nM which was higher when comparing with the PBS results. This result was attributed to higher protein content of serum containing medium. Proteins in serum can create biofouling on the surface and affect the sensing distance. The saturation point was at 10 μM antigen concentration, which was the same with the saturation point in PBS.

The work in this thesis can be extended for some further investigations. For instance, sensitivity of the biosensor can be increased by adjusting antibody orientation. The system can be integrated onto a microfluidic system to minimize the sample volume and to provide a more controllable detection.

REFERENCES

Ahirwar, Rajesh, Shilpi Bariar, Abitha Balakrishnan, and Pradip Nahar. (2015). 'BSA Blocking in Enzyme-Linked Immunosorbent Assays Is a Non-Mandatory Step: A Perspective Study on Mechanism of BSA Blocking in Common ELISA Protocols'. *RSC Advances*.

Ali, Jazib, Jawayria Najeeb, Muhammad Asim Ali, Muhammad Farhan Aslam, and Ali Raza. (2017). 'Biosensors: Their Fundamentals, Designs, Types and Most Recent Impactful Applications: A Review'. *Journal of Biosensors & Bioelectronics* 08 (01).

Balamurugan, Subramanian, Kathryn M. Mayer, Seunghyun Lee, Steven A. Soper, Jason H. Hafner, and David A. Spivak. (2013). 'Nanostructure Shape Effects on Response of Plasmonic Aptamer Sensors'. *Journal of Molecular Recognition*.

Bart, Jacob, Roald Tiggelaar, Menglong Yang, Stefan Schlautmann, Han Zuilhof, and Han Gardeniers. (2009). 'Room-Temperature Intermediate Layer Bonding for Microfluidic Devices'. *Lab on a Chip*.

Battersby, B.J., A. Chen, D. Kozak, and M. Trau. (2012). 'Biosensors for Disease Biomarker Detection'. *Biosensors for Medical Applications*, 191–216.

Bhalla, Nikhil, Pawan Jolly, Nello Formisano, and Pedro Estrela. (2016). 'Introduction to Biosensors'. *Essays in Biochemistry* 60 (1): 1–8.

Cao, Jie, Tong Sun, and Kenneth T.V. Grattan. (2014). 'Gold Nanorod-Based Localized Surface Plasmon Resonance Biosensors: A Review'. *Sensors and Actuators, B: Chemical* 195: 332–51.

Chen, Aicheng, and Sanghamitra Chatterjee. (2013). 'Nanomaterials Based Electrochemical Sensors for Biomedical Applications'. *Chemical Society Reviews* 42 (12): 5425–38.

Chen, Shenna, Qian Zhao, Lingyang Zhang, Linqian Wang, Yunlong Zeng, and Haowen Huang. (2015). 'Combined Detection of Breast Cancer Biomarkers Based on Plasmonic Sensor of Gold Nanorods'. *Sensors and Actuators, B: Chemical* 221: 1391–97.

Clark, Leland C., and Champ Lyons. (1962). 'ELECTRODE SYSTEMS FOR CONTINUOUS MONITORING IN CARDIOVASCULAR SURGERY'. *Annals of the New York Academy of Sciences*.

Ercole, C., M. Del Gallo, L. Mosiello, S. Baccella, and A. Lepidi. (2003). 'Escherichia Coli Detection in Vegetable Food by a Potentiometric Biosensor'. *Sensors and Actuators, B: Chemical* 91 (1–3): 163–68.

Erickson, David, Sudeep Mandal, Allen H.J. Yang, and Bernardo Cordovez. (2008). 'Nanobiosensors: Optofluidic, Electrical and Mechanical Approaches to Biomolecular Detection at the Nanoscale'. *Microfluidics and Nanofluidics* 4 (1–2): 33–52.

Ermiş, Nihal, Lokman Uzun, and Adil Denizli. (2017). 'Preparation of Molecularly Imprinted Electrochemical Sensor for L-Phenylalanine Detection and Its Application'. *Journal of Electroanalytical Chemistry*.

Gnoth, C., and S. Johnson. (2014). 'Strips of Hope: Accuracy of Home Pregnancy Tests and New Developments'. *Geburtshilfe Und Frauenheilkunde*.

Gobi, K. Vengatajalabathy, Chiwa Kataoka, and Norio Miura. (2005). 'Surface Plasmon Resonance Detection of Endocrine Disruptors Using Immunoprobes Based on Self-Assembled Monolayers'. In *Sensors and Actuators, B: Chemical*.

Gole, Anand, and Catherine J. Murphy. (2005). 'Biotin-Streptavidin-Induced Aggregation of Gold Nanorods: Tuning Rod-Rod Orientation'. *Langmuir*.

Grabinski, Christin, Nicole Schaeublin, Andy Wijaya, Helen D Couto, Salmaan H Baxamusa, Kimberly Hamad-schifferli, and Saber M Hussain. (2011). 'Effect of GNR Surface Chemistry on Cellular Response'. *ACS Nano* 5 (4): 2870–79.

Harder, P., M. Grunze, R. Dahint, G. M. Whitesides, and P. E. Laibinis. (1998). 'Molecular Conformation in Oligo(Ethylene Glycol)-Terminated Self-Assembled Monolayers on Gold and Silver Surfaces Determines Their Ability to Resist Protein Adsorption'. *Journal of Physical Chemistry B*.

He, X., S. P. Wang, Y. F. Zhou, C. M. Huang, S. B. Ning, and S. J. Lvq. (2017). 'A Novel Method to Detect Circulating Antigens of Schistosoma Japonicum Using a Gold Nanorod Optical Sensor'. *Tropical Biomedicine* 34 (1): 180–90.

Hoft, Rainer C., Michael J. Ford, Andrew M. McDonagh, and Michael B. Cortie. (2007). 'Adsorption of Amine Compounds on the Au(111) Surface: A Density Functional Study'. *Journal of Physical Chemistry C*.

Huang, Xiaohua, Prashant K. Jain, Ivan H. El-Sayed, and Mostafa A. El-Sayed. (2007). 'Gold Nanoparticles: Interesting Optical Properties and Recent Applications in Cancer Diagnostics and Therapy'. *Nanomedicine* 2 (5): 681–93.

Huang, Xiaohua, Svetlana Neretina, and Mostafa A. El-Sayed. (2009). 'Gold Nanorods: From Synthesis and Properties to Biological and Biomedical Applications'. *Advanced Materials* 21 (48): 4880–4910.

Jana, N. R., L. Gearheart, and C. J. Murphy. (2001). 'Seed-Mediated Growth Approach for Shape-Controlled Synthesis of Spheroidal and Rod-like Gold Nanoparticles Using a Surfactant Template'. *Advanced Materials*.

Jia, Yan Peng, Kun Shi, Jin Feng Liao, Jin Rong Peng, Ying Hao, Ying Qu, Li Juan Chen, et al. (2020). 'Effects of Cetyltrimethylammonium Bromide on the Toxicity of Gold Nanorods Both In Vitro and In Vivo: Molecular Origin of Cytotoxicity and Inflammation'. *Small Methods* 4 (3): 1–11.

Keusgen, Michael. (2002). 'Biosensors: New Approaches in Drug Discovery'. *Naturwissenschaften* 89 (10): 433–44.

Kim, Hyung Min, Seung Min Jin, Seok Kee Lee, Min Gon Kim, and Yong Beom Shin. (2009). 'Detection of Biomolecular Binding through Enhancement of Localized Surface Plasmon Resonance (LSPR) by Gold Nanoparticles'. *Sensors*.

Kirsch, Jeffrey, Christian Siltanen, Qing Zhou, Alexander Revzin, and Aleksandr Simonian. (2013). 'Biosensor Technology: Recent Advances in Threat Agent Detection and Medicine'. *Chemical Society Reviews* 42 (22): 8733–68.

Kosuda, K. M., J. M. Bingham, K. L. Wustholz, and R. P. Van Duyne. (2011). 'Nanostructures and Surface-Enhanced Raman Spectroscopy'. *Comprehensive Nanoscience and Technology* 1–5: 263–301.

Lavín, Álvaro, Jesús de Vicente, Miguel Holgado, María F. Laguna, Rafael Casquel, Beatriz Santamaría, María Victoria Maigler, Ana L. Hernández, and Yolanda Ramírez. (2018). 'On the Determination of Uncertainty and Limit of Detection in Label-Free Biosensors'. *Sensors (Switzerland).*

Lee, Thomas Ming Hung. (2008). 'Over-the-Counter Biosensors: Past, Present, and Future'. *Sensors* 8 (9): 5535–59.

Liao, Hongwei, Colleen L. Nehl, and Jason H. Hafner. (2006). 'Biomedical Applications of Plasmon Resonant Metal Nanoparticles'. *Nanomedicine* 1 (2): 201–8.

Malekzad, Hedieh, Parham Sahandi Zangabad, Hamed Mirshekari, Mahdi Karimi, and Michael R. Hamblin. (2017). 'Noble Metal Nanoparticles in Biosensors: Recent Studies and Applications'. *Nanotechnology Reviews* 6 (3): 301–29.

Mannelli, Ilaria, and M. Pilar Marco. (2010). 'Recent Advances in Analytical and Bioanalysis Applications of Noble Metal Nanorods'. *Analytical and Bioanalytical Chemistry* 398 (6): 2451–69.

Marinakos, Stella M, Sihai Chen, and Ashutosh Chilkoti. (2007). ‘Plasmonic Detection of a Model Analyte in Serum by a Gold Nanorod Sensor’ 79 (14): 5278–83.

Mayer, Kathryn M., and Jason H. Hafner. (2011). ‘Localized Surface Plasmon Resonance Sensors’. *Chemical Reviews* 111 (6): 3828–57.

Mayer, Kathryn M., Seunghyun Lee, Hongwei Liao, Betty C. Rostro, Amaris Fuentes, Peter T. Scully, Colleen L. Nehl, and Jason H. Hafner. (2008). ‘A Label-Free Immunoassay Based upon Localized Surface Plasmon Resonance of Gold Nanorods’. *ACS Nano*.

Mehrotra, Parikha. (2016). ‘Biosensors and Their Applications - A Review’. *Journal of Oral Biology and Craniofacial Research* 6 (2): 153–59.

Nehl, Colleen L., Hongwei Liao, and Jason H. Hafner. (2006). ‘Optical Properties of Star-Shaped Gold Nanoparticles’. *Nano Letters*.

Nie, Shuming, Yun Xing, Gloria J Kim, and Jonathan W Simons. (2007). ‘Nanotechnology Applications in Cancer’.

Niidome, Takuro, Masato Yamagata, Yuri Okamoto, Yasuyuki Akiyama, Hironobu Takahashi, Takahito Kawano, Yoshiki Katayama, and Yasuro Niidome. (2006). ‘PEG-Modified Gold Nanorods with a Stealth Character for in Vivo Applications’. *Journal of Controlled Release* 114 (3): 343–47.

Nikoobakht, Babak, and Mostafa A. El-Sayed. (2001). ‘Evidence for Bilayer Assembly of Cationic Surfactants on the Surface of Gold Nanorods’. *Langmuir*.

Nikoobakht, Babak, and Mostafa A. El-Sayed. (2003). ‘Preparation and Growth Mechanism of Gold Nanorods (NRs) Using Seed-Mediated Growth Method’. *Chemistry of Materials*.

Onaciu, Anca, Cornelia Braicu, Alina Andreea Zimta, Alin Moldovan, Rares Stiufiuc, Mihail Buse, Cristina Ciocan, Smaranda Buduru, and Ioana Berindan-Neagoe. (2019). ‘Gold Nanorods: From Anisotropy to Opportunity. An Evolution Update’. *Nanomedicine* 14 (9): 1203–26.

Pai, Jing Hong, Chih Tsung Yang, Hung Yao Hsu, A. Bruce Wedding, and Benjamin Thierry. (2017). ‘Development of a Simplified Approach for the Fabrication of Localised Surface Plasmon Resonance Sensors Based on Gold Nanorods Functionalized Using Mixed Polyethylene Glycol Layers’. *Analytica Chimica Acta* 974: 87–92.

Peixoto, Linus Pauling F., Jacqueline F.L. Santos, and Gustavo F.S. Andrade. (2019). ‘Plasmonic Nanobiosensor Based on Au Nanorods with Improved Sensitivity: A Comparative Study for Two Different Configurations’. *Analytica Chimica Acta* 1084: 71–77.

Pejcic, Bobby, Roland De Marco, and Gordon Parkinson. (2006). 'The Role of Biosensors in the Detection of Emerging Infectious Diseases'. *Analyst* 131 (10): 1079–90.

Pissuwan, Dakrong, Stella M. Valenzuela, and Michael B. Cortie. (2008). 'Prospects for Gold Nanorod Particles in Diagnostic and Therapeutic Applications'. *Biotechnology and Genetic Engineering Reviews* 25 (1): 93–112.

Radulescu, Maria Cristina, Bogdan Bucur, Madalina Petruta Bucur, and Gabriel Lucian Radu. (2014). 'Bienzymatic Biosensor for Rapid Detection of Aspartame by Flow Injection Analysis'. *Sensors (Switzerland)* 14 (1): 1028–38.

Sabu, Chinnu, T. K. Henna, V. R. Raphey, K. P. Nivitha, and K. Pramod. (2019). 'Advanced Biosensors for Glucose and Insulin'. *Biosensors and Bioelectronics* 141 (January): 111201.

Seol, Seung Kwon, Daeho Kim, Sunshin Jung, Won Suk Chang, and Ji Tae Kim. (2013). 'One-Step Synthesis of PEG-Coated Gold Nanoparticles by Rapid Microwave Heating'. *Journal of Nanomaterials*.

Sepúlveda, Borja, Paula C. Angelomé, Laura M. Lechuga, and Luis M. Liz-Marzán. (2009). 'LSPR-Based Nanobiosensors'. *Nano Today* 4 (3): 244–51.

Sharma, Vivek, Kyoungweon Park, and Mohan Srinivasarao. (2009). 'Colloidal Dispersion of Gold Nanorods: Historical Background, Optical Properties, Seed-Mediated Synthesis, Shape Separation and Self-Assembly'. *Materials Science and Engineering R: Reports* 65 (1–3): 1–38.

Singh, Anu, H. N. Verma, and Kavita Arora. (2014). 'Surface Plasmon Resonance Based Label-Free Detection of Salmonella Using DNA Self Assembly'. *Applied Biochemistry and Biotechnology*.

Soper, Steven A, Kathlynn Brown, Andrew Ellington, Bruno Frazier, Guillermo Garcia-manero, Vincent Gau, Steven I Gutman, et al. (2006). 'Point-of-Care Biosensor Systems for Cancer Diagnostics / Prognostics' 21: 1932–42.

Tan, Shu Fen, Utkarsh Anand, and Utkur Mirsaidov. (2017). 'Interactions and Attachment Pathways between Functionalized Gold Nanorods'. *ACS Nano* 11 (2): 1633–40.

Tothill, Ibtisam E. (2009). 'Biosensors for Cancer Markers Diagnosis'. *Seminars in Cell and Developmental Biology* 20 (1): 55–62.

Truong, Phuoc Long, Cuong Cao, Sungho Park, Moonil Kim, and Sang Jun Sim. (2011). 'A New Method for Non-Labeling Attomolar Detection of Diseases Based on an Individual Gold Nanorod Immunosensor'. *Lab on a Chip* 11 (15): 2591–97.

Truong, Phuoc Long, Byung Woo Kim, and Sang Jun Sim. (2012). 'Rational Aspect Ratio and Suitable Antibody Coverage of Gold Nanorod for Ultra-Sensitive Detection of a Cancer Biomarker'. *Lab on a Chip* 12 (6): 1102–9.

Underwood, Sylvia, and Paul Mulvaney. (1994). 'Effect of the Solution Refractive Index on the Color of Gold Colloids'. *Langmuir*.

Unser, Sarah, Ian Bruzas, Jie He, and Laura Sagle. (2015). 'Localized Surface Plasmon Resonance Biosensing: Current Challenges and Approaches'. *Sensors (Switzerland)* 15 (7): 15684–716.

Vigderman, Leonid, Bishnu P. Khanal, and Eugene R. Zubarev. (2012). 'Functional Gold Nanorods: Synthesis, Self-Assembly, and Sensing Applications'. *Advanced Materials* 24 (36): 4811–41.

Vo-Dinh, Tuan, and Brian Cullum. (2000). 'Biosensors and Biochips: Advances in Biological and Medical Diagnostics'. *Fresenius' Journal of Analytical Chemistry* 366 (6–7): 540–51.

Vonnemann, Jonathan, Nicolas Beziere, Christoph Böttcher, Sebastian B. Riese, Christian Kuehne, Jens Dernedde, Kai Licha, et al. (2014). 'Polyglycerolsulfate Functionalized Gold Nanorods as Optoacoustic Signal Nanoamplifiers for in Vivo Bioimaging of Rheumatoid Arthritis'. *Theranostics*.

Wang, Xiaohui, Yuan Li, Huafen Wang, Qiuxia Fu, Jianchun Peng, Yingli Wang, Juan Du, Yong Zhou, and Linsheng Zhan. (2010). 'Gold Nanorod-Based Localized Surface Plasmon Resonance Biosensor for Sensitive Detection of Hepatitis B Virus in Buffer, Blood Serum and Plasma'. *Biosensors and Bioelectronics* 26 (2): 404–10.

Wang, Yanyan, and Liang Tang. (2013). 'Chemisorption Assembly of Au Nanorods on Mercaptosilanized Glass Substrate for Label-Free Nanoplasmon Biochip'. *Analytica Chimica Acta* 796: 122–29.

WHO. (2018). 'Latest Global Cancer Data: Cancer Burden Rises to 18.1 Million New Cases and 9.6 Million Cancer Deaths in 2018'. *Journal of the Medical Society of Toho University*.

Willets, Katherine A., and Richard P. Van Duyne. (2007). 'Localized Surface Plasmon Resonance Spectroscopy and Sensing'. *Annual Review of Physical Chemistry* 58 (1): 267–97.

Yan, Binghai, Yang Yang, and Yongchang Wang. (2003). 'Comment on "Simulation of the Optical Absorption Spectra of Gold Nanorods as a Function of Their Aspect Ratio and the Effect of the Medium Dielectric Constant"'. *Journal of Physical Chemistry B* 107 (34): 9159.

Zhou, Jie, Zhonglin Cao, Nishtha Panwar, Rui Hu, Xiaomei Wang, Junle Qu, Swee Chuan Tjin, Gaixia Xu, and Ken Tye Yong. (2017). 'Functionalized Gold Nanorods for Nanomedicine: Past, Present and Future'. *Coordination Chemistry Reviews* 352: 15–66.

Zhou, Yan, Yi Fang, and Ramaraja P. Ramasamy. (2019). 'Non-Covalent Functionalization of Carbon Nanotubes for Electrochemical Biosensor Development'. *Sensors (Switzerland)* 19 (2).